Numerical analysis of relaxed micromagnetics by penalised finite elements

Carsten Carstensen, Andreas Prohl

Mathematisches Seminar, Christian-Albrechts-Universität zu Kiel,
Ludewig-Meyn-Strasse 4, 24098 Kiel, Germany; e-mail: {cc, apr}@numerik.uni-kiel.de

Summary. Some micromagnetic phenomena in rigid (ferro-)magnetic materials can be modelled by a non-convex minimisation problem. Typically, minimising sequences develop finer and finer oscillations and their weak limits do not attain the infimal energy. Solutions exist in a generalised sense and the observed microstructure can be described in terms of Young measures. A relaxation by convexifying the energy density resolves the essential macroscopic information. The numerical analysis of the relaxed problem faces convex but degenerated energy functionals in a setting similar to mixed finite element formulations. The lowest order conforming finite element schemes appear instable and nonconforming finite element methods are proposed. An a priori and a posteriori error analysis is presented for a penalised version of the side-restriction that the modulus of the magnetic field is bounded pointwise. Residual-based adaptive algorithms are proposed and experimentally shown to be efficient.

Mathematics Subject Classification (1991): 64M07, 65K10, 65N30, 73C50, 73S10, 65N15, 65N30, 65N50

1. Introduction

This paper concerns the numerical treatment of the Euler-Lagrange equations of a degenerated convexified minimisation problem for a magnetisation $\mathbf{m}$ and a potential u: Given $\mathbf{f} \in L^2(\omega)^2$ and bounded Lipschitz domains $\omega \subset\subset \Omega \subset\subset \mathbb{R}^2$, seek $u \in H_0^1(\Omega)$ and $\mathbf{m} \in L^2(\omega)^2$ with $|\mathbf{m}| \leq 1$ almost everywhere in ω which satisfy

---
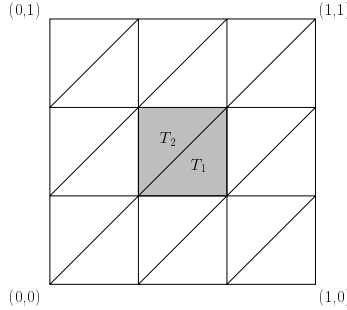
Correspondence to: C. Carstensen

Fig. 1. A coarse grid where a non-zero magnetisation on $T_1 \cup T_2$ provides a solution to the homogeneous discrete problem

$$(1.1) \qquad \int_\Omega \nabla u \cdot \nabla w \, dx = \int_\omega \mathbf{m} \cdot \nabla w \, dx,$$

$$(1.2) \qquad \int_\omega (\mathbf{f} - \nabla u) \cdot (\boldsymbol{\mu} - \mathbf{m}) dx \le \int_\omega (\phi^{**}(\boldsymbol{\mu}) - \phi^{**}(\mathbf{m})) dx,$$

for all $w \in H_0^1(\Omega)$ and $\boldsymbol{\mu} \in L^2(\omega)^2$ with $|\boldsymbol{\mu}| \le 1$ almost everywhere in ω. The mathematical model is explained in detail in Sect. 2 where we prove uniqueness of solutions in the uniaxial case $\phi^{**}(\mathbf{m}) = (\mathbf{m} \cdot \mathbf{e}_\perp)^2/2$ for perpendicular unit vectors $\mathbf{e}$ and $\mathbf{e}_\perp$. $\mathbf{e}$ is called the easy axis because of $\phi^{**}(t\,\mathbf{e}) = 0$ and $D\phi^{**}(t\,\mathbf{e}) = 0$ for all $t \in \mathbb{R}$. The physical setting and the relation of (1.1)–(1.2) to major activities in computational micromagnetics literature will be discussed in Sect. 2 as well. For the sake of this introduction, we focus on the mathematical aspects of the numerical analysis of (1.1)–(1.2) which we found interesting.

At first glance, it is surprising that a natural conforming discretisation which replaces $H_0^1(\Omega)$ by a standard conforming $P1$-finite element scheme and $L^2(\omega)^2$ by piecewise constants finite elements fails, e.g., for the standard mesh $\mathcal{T}$ of Fig. 1 on the unit square.

Example 1.1. Let $\mathbf{m}_h|_{T_j} = (-1)^j (1,1)/\sqrt{2}$, $\omega = \text{int}(T_1 \cup T_2) = (1/3, 2/3)^2 \subset \Omega = (0,1)^2$ and notice by direct calculation that $\int_\omega \mathbf{m}_h \cdot \nabla \varphi_z \, dx = 0$ for each hat function φ_z (the nodal basis function for conforming $\mathcal{T}$-piecewise affine finite elements). In the uniaxial case with $\mathbf{e} = (1,1)/\sqrt{2}$ we have $\phi^{**}(\mathbf{m}_h) = 0$. Hence, $t\,\mathbf{m}_h$ and $u_h = 0$ satisfy the discrete version of (1.1)-(1.2) for $\mathbf{f} = 0$ and any $t \in \mathbb{R}$ with $|t| \le 1$. A discrete Helmholtz decomposition (cf. [AF]) shows why: $\mathbf{m}_h$ is the piecewise curl of a nonconforming hat function ψ_z ($\psi_z = 1$ on $T_1 \cap T_2$ and zero at midpoints of other edges of $\partial\omega$) and is parallel to $\mathbf{e}$. One remedy in this particular situation is to change the mesh by taking the other diagonals in Fig. 1 or, equivalently, transform the situation to $\mathbf{e} = (1,-1)/\sqrt{2}$.

At second glance, ignoring $\mathbf{f}$, ϕ^{**}, and the saturation condition $|\mathbf{m}| \leq 1$, the resulting system in (1.1)-(1.2) is a mixed system and so a conforming $P1$-$Q0$-finite element discretisation may expected to be instable, but non-conforming $P1$-finite elements may be stable. The uniqueness of discrete solutions for Crouzeix-Raviart elements will be proved in Sect. 3. In Sect. 4 below, we will study what quantities can be controlled and at which convergence order for the lowest order conforming and nonconforming method.

As the side restriction $|\mathbf{m}| \leq 1$ in (1.2) yields a variational inequality, optimal convergence results cannot be expected. If $\varepsilon > 0$ is a small penalty parameter to penalise $|\mathbf{m}| \leq 1$ we prove $\mathcal{O}(\varepsilon + \sqrt{h})$ for the conforming and $\mathcal{O}(\varepsilon + h)$ for the nonconforming lowest order finite elements for some error terms as the piecewise derivatives of $u - u_h$ and the components $(\mathbf{m} - \mathbf{m}_h) \cdot \mathbf{e}_\perp$. We regard the estimates $\mathcal{O}(\varepsilon + h)$ as being optimal in ε and in h.

It should be emphasised that the estimates are optimal in case that ϕ^{**} is uniformly convex. Hence, we may say that the penalisation of the side restriction $|\mathbf{m}| \leq 1$ is treated in an optimal way. It is the degenerated not strictly convex part of ϕ^{**} that causes poorer estimates as in convexified two-well problems [CP1, CP2].

The underlying assumption of smooth solutions is an open question and it may be believed that the boundary of the set $\{x \in \omega : |\mathbf{m}| = 1\}$ (unknown a priori) gives rise to non-smooth solutions. Here, self-refining adaptive finite element schemes might be an efficient tool and hence we study residual-based a posteriori error estimates in Sect. 5. They are either efficient (optimal weights of local mesh-sizes) or reliable (in the sense that no regularity assumption on the unknown solution is made) but not both. In Sect. 6 we report on numerical examples to monitor the optimality of the estimates.

The notation for Lebesgue spaces is standard, e.g., $\| \cdot \|_{p,\Omega} := \| \cdot \|_{L^p(\Omega)}$ denotes the norm in (any power of) $L^p(\Omega)$ and $H^s(\Omega)$ are the usual Sobolev spaces ($s \in \mathbb{R}$) for a bounded Lipschitz domain Ω with boundary Γ. Let $\| \cdot \|_{k,2,\omega} := \| \cdot \|_{H^k(\omega)}$ and $| \cdot |_{H^k(\omega)}$ denote the norm and semi-norm in $H^k(\omega)$ for $\omega \subseteq \Omega$ and an integer k.

2. Mathematical model

Micromagnetic phenomena in a rigid (ferro-)magnetic body $\omega \subset \mathbb{R}^d$, $d = 2, 3$, are described in terms of the magnetisation $\mathbf{m} : \omega \to \mathbb{R}^d$ and the scalar potential $u : \Omega \to \mathbb{R}$ in the larger simply connected domain $\Omega \subset \mathbb{R}^d$ that surrounds $\omega \subset \Omega$.

The classical model of Weiss, Landau, and Lifshitz [B] assumes the energy $E(\mathbf{m})$ to be a sum of exchange, anisotropic, exterior (i.e., from a given magnetisation $\mathbf{f}$) and magnetostatic energies

$$E(\mathbf{m}) = \alpha \int_\omega |\nabla \mathbf{m}|^2 \, dx + \int_\omega \phi(\mathbf{m}) \, dx$$

(2.1)
$$- \int_\omega \mathbf{f} \cdot \mathbf{m} \, dx + \frac{1}{2} \int_\Omega |\nabla u|^2 \, dx.$$

For each $\mathbf{m} \in L^2(\omega)^2$ there exists a unique $u \in H_0^1(\Omega)$ that satisfies Maxwell's equations which result in

(2.2) $$-\Delta u + \operatorname{div}(\mathbf{m}\chi_\omega) = 0 \quad \text{in } H^{-1}(\Omega).$$

Here, χ_ω is the characteristic function of the set ω, i.e., $\chi_\omega(x) = 1$ if $x \in \omega$ and $\chi_\omega(x) = 0$ if not.

In many physical applications, $\Omega = \mathbb{R}^d$ is the full space and proper radiation conditions are required as boundary conditions at infinity. In this paper we focus on a bounded domain Ω where the interface conditions state that the magnetic flux H is perpendicular to the wall $\partial\Omega$ which yields $H \cdot t = \partial u / \partial s = 0$ with the tangential unit vector t and derivative $\partial/\partial s$ with respect to the arc-length along $\partial\Omega$. Thus, u is constant on the connected boundary $\partial\Omega$ and so we suppose without loss of generality, $u = 0$, i.e., $u \in H_0^1(\Omega)$.

Below a critical temperature (Curie point), the modulus of $\mathbf{m}$ is fixed pointwise and (assuming constant temperature) we suppose

(2.3) $$|\mathbf{m}| = 1 \quad \text{almost everywhere in } \omega.$$

Then, the **Minimisation Problem** (M_α) reads as follows: *Given* $\mathbf{f} \in L^2(\omega)^2$ *minimise the energy (2.1) subject to (2.2) and (2.3).*

For small positive α, the minimisers of (M_α) show fine oscillations of an α-depending length scale that is much smaller than a realistic mesh-size. Macroscopic phenomena depend very much on the remaining lower order terms. Following [ADS, T], we therefore study a relaxation of the limit case (M_0) in this paper, where the exchange energy $\alpha \int_\omega |\nabla \mathbf{m}|^2 \, dx$ is neglected in (2.1), i.e., $\alpha = 0$.

Typically, $\phi(\mathbf{m}) \geq 0$ has a finite number of zero states related by some symmetry group, e.g., ϕ even and $\phi(\mathbf{m}) = 0$ if and only if $\mathbf{m} = \pm \mathbf{e}$ for some unit vector $\mathbf{e}$ (the easy axis). It is known in this case that Problem (M_0) may have no classical solution [JK]: in general, the infimal energy is not attained. Minimising sequences exist, are bounded, contain weakly converging subsequences, but show higher and higher oscillations which prohibit strong convergence. The weak limit does describe the macroscopic magnetisation but does not characterise the microscopic mechanism of energy minimisation.

Remark 2.1. For a survey of the state of the art in micromagnetics, we refer to the recent monograph of Hubert and Schäfer [HS] and the works quoted therein, or related journals such as IEEE TRANSACTIONS ON MAGNET-ICS. In most of these contributions, problem (M_α) is addressed numerically by a finite element scheme similar to the conforming discretisation of Sect. 3. For an exchange constant $\alpha \approx 10^{-11} J/m$, observed micromagnetic phenomena in samples of permalloy (like Bloch walls) then show a characteristic length of approximately $6nm$. Physicists are interested in those fine structures and hence are restricted to very small magnets, where e.g., ω is a rectangle of size $1\mu m \times 2\mu m$, according to limited computer power. Adaptive schemes are in use to allow three-dimensional calculations. However, the numerical results depends very much on starting values for the iterative solver (cf. Sect. 6 for our strategy in the same spirit). The mathematical foundations of those numerical experiments still have to be developed, and this work is devoted to contribute in this direction. Consequently, the main motivation in this paper is to understand the limit problem (M_0) and its sound numerical analysis before addressing its perturbation (M_α).

From a variational point of view [D], model (M_0) has to be generalised to allow measure valued solutions [P1, R, T] and be well-posed. On the other hand, the main interest is often on the averaged (macroscopic) magnetisation properties of the ferromagnet. To obtain those informations it is sufficient to consider a modified minimisation problem (R). The relaxation of the present example is analysed in [ADS] and essentially means a convexification of ϕ and of (2.3). Let $\varphi(\mathbf{m})$ denote the lower convex envelope $\phi^{**}(\mathbf{m})$ of ϕ if $|\mathbf{m}| \leq 1$ and $\varphi(\mathbf{m}) = \infty$ if not. The lower convex envelope ϕ^{**} is the largest convex function below ϕ. Then, the **Relaxed Problem (R)** reads: *Seek a minimiser $\mathbf{m} \in L^2(\omega)$ of the relaxed energy*

$$(2.4) \qquad RE(\mathbf{m}) = \int_\omega \varphi(\mathbf{m})dx - \int_\omega \mathbf{f} \cdot \mathbf{m}dx + \frac{1}{2}\int_\Omega |\nabla u|^2 \, dx$$

subject to (2.2).

Since minimising sequences of (R) have bounded magnetisation and so a bounded potential, there exist weakly convergent subsequences. Owing to the convexification, the relaxed energy functional RE is sequentially weakly lower semi-continuous and there exist solutions of (R) [ADS]. Each solution of (R) solves the Euler-Lagrange equations (1.1)-(1.2) and, if we involve a further Lagrange multiplier with respect to the constraint $|\mathbf{m}| \leq 1$, solves **Problem (P)**: *Seek $u \in H_0^1(\Omega)$, $\mathbf{m} \in L^2(\omega)^2$, and $\lambda \in L^2(\omega)$ satisfying*

$$(2.5) \qquad \int_\Omega \nabla u \cdot \nabla w \, dx = \int_\omega \mathbf{m} \cdot \nabla w \, dx \quad (w \in H_0^1(\Omega)),$$

$$(2.6) \qquad \nabla u + D\phi^{**}(\mathbf{m}) + \lambda\mathbf{m} = \mathbf{f} \quad \text{a.e. in } \omega,$$

(2.7) $0 \leq \lambda, \quad |\mathbf{m}| \leq 1, \quad$ and $\quad \lambda(1 - |\mathbf{m}|)_+ = 0 \quad$ a.e. in ω.

Here, $(s)_+ := \max\{s, 0\}$ denotes the non-negative part and the last condition in (2.7) states that $\lambda \neq 0$ is possible only for $|\mathbf{m}| = 1$ as a consequence of $\lambda\mathbf{m} \in \partial\psi(\mathbf{m})$ for the convex characteristic functional $\psi : \mathbb{R}^2 \to [0, \infty]$ defined by $\psi(\mathbf{m}) = 0$ if $|\mathbf{m}| \leq 1$ and $\psi(\mathbf{m}) = \infty$ if not.

Remark 2.2. According to (2.5), the stray-field $\nabla u = \mathcal{L}(\chi_\omega\mathbf{m})$, where $\mathcal{L}(\mathbf{m}) = \nabla\Delta_D^{-1}\mathrm{div}\,(\chi_\omega\mathbf{m})$ and $\Delta_D^{-1} : H^{-1}(\Omega) \to H_0^1(\Omega)$ denotes the solution operator for the Laplace problem with homogeneous Dirichlet boundary data. Then, the Euler-Lagrange equation of (2.4) reads $\mathcal{L}^\star\mathcal{L}\mathbf{m} + D\phi^{\star\star}(\mathbf{m}) + \lambda\mathbf{m} = \mathbf{f}$ in $L^2(\omega)^2$. One can prove that this indeed implies (2.6).

Remark 2.3. The oscillations of minimizing sequences of Problem (P) cannot be observed in the Relaxed Problem (R) with a (possibly) smooth solution $\mathbf{m}$ but can be computed from it. For instance, the Young measure generated by minimising sequences is

(2.8) $\nu_x = \lambda(\mathbf{m})\delta_{\mathbf{m}^+(\mathbf{m})} + (1 - \lambda(\mathbf{m}))\delta_{\mathbf{m}^-(\mathbf{m})},$

$\mathbf{m}^\pm(\mathbf{m}) := \pm(1 - (\mathbf{m} \cdot \mathbf{e}_\perp)^2)^{1/2}\mathbf{e} + (\mathbf{m} \cdot \mathbf{e}_\perp)\mathbf{e}_\perp,$ and

(2.9) $\lambda(\mathbf{m}) := \dfrac{1}{2} + \dfrac{\mathbf{m} \cdot \mathbf{e}}{2(1 - (\mathbf{m} \cdot \mathbf{e}_\perp)^2)^{1/2}}$

in the uniaxial case with easy axis $\mathbf{e} \in \mathbb{R}^2$ (see [ADS] for a proof). We refer to [LM, Pr] for a direct minimisation approach for $\mathbf{f} = 0$.

As shown in [ADS, Thm 4.2], any solution of (R) solves (P) and, in particular, Problem (P) has solutions. Their uniqueness is claimed in a misleading way in [P2, P3] and is discussed in a simplified setting in [ADS]. Therefore, we conclude this section with a clarification of uniqueness in the present model: for the important uniaxial case there exists a unique solution while, in general, the number of solutions may be infinite.

Theorem 2.1. *In the uniaxial case, where $\phi^{**}(\mathbf{m}) = \frac{1}{2}(\mathbf{m} \cdot \mathbf{e}_\perp)^2$ for some unit vector $\mathbf{e} \in \mathbb{R}^2$ and its normal $\mathbf{e}_\perp$, there exists only one solution in Problem (P) and in Problem (R). In general, there are infinitely many minimisers in the cubic case, where $\phi(\mathbf{m}) = m_1^2 m_2^2$ for $\mathbf{m} = (m_1, m_2) \in \mathbb{R}^2$.*

Proof. Suppose $(\mathbf{m}_j, \lambda_j, u_j)$ solves (P) for $j = 1, 2$ and denote $e := u_2 - u_1$ and $\boldsymbol{\delta} = \mathbf{m}_2 - \mathbf{m}_1$. According to (2.5), we have

(2.10) $\displaystyle\int_\omega \nabla e \cdot \boldsymbol{\delta}\, dx = |e|_{1,2,\Omega}^2.$

From the monotonicity of the subgradients we infer from $\lambda_j \mathbf{m}_j \in \partial \psi(\mathbf{m}_j)$ that $\lambda_j \mathbf{m}_j (\mathbf{m}_{j+1} - \mathbf{m}_j) \leq 0$ for $j = 1, 2$ and $\mathbf{m}_3 := \mathbf{m}_1$. This shows $0 \leq (\lambda_2 \mathbf{m}_2 - \lambda_1 \mathbf{m}_1) \cdot \boldsymbol{\delta}$ almost everywhere in ω. Similar arguments show $0 \leq (D\phi^{**}(\mathbf{m}_2) - D\phi^{**}(\mathbf{m}_1)) \cdot \boldsymbol{\delta}$ and we deduce with (2.6) and (2.10) that all the three terms in

$$\| \nabla e \|_{2,\Omega}^2 + \int_\omega (D\phi^{**}(\mathbf{m}_2) - D\phi^{**}(\mathbf{m}_1)) \cdot \boldsymbol{\delta} \, dx$$

(2.11) $$+ \int_\omega (\lambda_2 \mathbf{m}_2 - \lambda_1 \mathbf{m}_1) \cdot \boldsymbol{\delta} \, dx = 0$$

are non-negative and hence vanish: $\mathbf{e} = 0$, $(\lambda_2 \mathbf{m}_2 - \lambda_1 \mathbf{m}_1) \cdot \boldsymbol{\delta} = 0$ and $(D\phi^{**}(\mathbf{m}_2) - D\phi^{**}(\mathbf{m}_1)) \cdot \boldsymbol{\delta} = 0$ almost everywhere.

In the uniaxial case $\phi^{**}(\mathbf{m}) = \frac{1}{2}(\mathbf{m} \cdot \mathbf{e}_\perp)^2$, we have $D\phi^{**}(\mathbf{m}) = (\mathbf{m} \cdot \mathbf{e}_\perp) \, \mathbf{e}_\perp$ and so infer

(2.12) $$0 = (D\phi^{**}(\mathbf{m}_2) - D\phi^{**}(\mathbf{m}_1)) \cdot \boldsymbol{\delta} = (\boldsymbol{\delta} \cdot \mathbf{e}_\perp)^2.$$

On the other hand, $\mathbf{e} = 0$ and (2.10) imply that $\boldsymbol{\delta}$ is divergence-free in the sense of distributions. This means div $\boldsymbol{\delta} = 0$ almost everywhere in ω but also $\boldsymbol{\delta} \cdot n = 0$ on the boundary $\partial \omega$ with unit normal vector n (in a weak sense according to the formula of integration by parts). Let us extend $\boldsymbol{\delta}$ by zero outside ω. Since the normal components are continuous on the boundary $\partial \omega$, the extended function $\boldsymbol{\delta}$ belongs to $H(\text{div}; \mathbb{R}^2)$ and is divergence-free. Hence, $\boldsymbol{\delta} = \text{curl}\, \eta := (\eta_{,2}, -\eta_{,1})$ for some $\eta \in H^1(\omega)$, cf. e.g., [GR, Theorem 3.1 on page 37]. Outside a ball that includes ω, $\boldsymbol{\delta} = 0$ and so η is constant there. Without loss of generality, $\eta = 0$ on the connectivity component γ_0 of the boundary $\partial \omega$ that includes ω.

Because of (2.12), $\nabla \eta$ is parallel to $\mathbf{e}$, i.e., the directional derivative of η in the direction $\mathbf{e}_\perp$ vanishes almost everywhere in ω. Since $\eta = 0$ on γ and is constant along almost all lines in parallel to $\mathbf{e}$ inside ω (and according to the extension of $\boldsymbol{\delta}$, η is constant in bounded components of $\mathbb{R}^2 \setminus \omega$) we deduce $\eta = 0$. This shows $\boldsymbol{\delta} = 0$ and even $\lambda_2 = \lambda_1$ by (2.6).

In the cubic case, the convexification ϕ^{**} of ϕ is zero for $\mathbf{m}$ equal to $(\pm 1, 0)$ and $(0, \pm 1)$. Consequently, ϕ^{**} vanishes on their convex hull and so, in particular, on the ball $B(0, 1/2)$. Given $\mathbf{f} = 0$, one solution with minimal zero energy is $\mathbf{m} = 0$, $u = 0$, $\lambda = 0$. However, for any smooth η with compact support in ω which is small (by scaling with a small factor), i.e., $|\nabla \eta| \leq 1/2$ almost everywhere in ω the functions $\mathbf{m} = \text{curl}\, \eta$, $u = 0$, and $\lambda = 0$ solve (P). This shows that there are infinitely many solutions in the cubic case.

3. Conforming and nonconforming discretisation and penalisation

In the first part of this section, we consider the lowest order conforming finite element method and show that it is *not* feasible. This favours the use of nonconforming finite element schemes for which we prove stability and optimal a priori error estimates.

For simplicity, let $\mathcal{T}$ be a regular triangulation of Ω and ω with polygonal boundary in the sense of Ciarlet [BS]; i.e., $\mathcal{T}$ is a finite partition of Ω in closed triangles such that two distinct T and T' in $\mathcal{T}$ are either disjoint, or $T \cup T'$ is a complete edge or a common node of both T and T'. We suppose that ω is covered exactly by the sub-triangulation $\mathcal{T}|_\omega = \{T \in \mathcal{T} : T \subset \overline{\omega}\}$.

Given $\mathcal{T}$, let $\mathcal{E}$ denote the set of all edges and $\mathcal{N}$ denote the set of all nodes in Ω; $\mathcal{N}$ is partitioned into free nodes in the interior $\mathcal{K} := \mathcal{N} \cap \omega$ and those on the outer boundary $\mathcal{N} \cap \partial\Omega$. The set of all midpoints of edges E in $\mathcal{E}$ is denoted by $\mathcal{M}$.

The class of lowest order finite element spaces under consideration is defined by

$$\mathcal{L}^0(\mathcal{T}|_\omega) := \{V \in L^\infty(\omega) : \ \forall T \in \mathcal{T}|_\omega, \ V|_T \text{ constant}\},$$
$$\mathcal{S}^1(\mathcal{T}) := \{V \in C(\Omega) : \ \forall T \in \mathcal{T}, V|_T \text{ affine}\},$$
$$\mathcal{S}^1_0(\mathcal{T}) := \{V \in \mathcal{S}^1(\mathcal{T}) : \ V = 0 \text{ on } \partial\Omega\},$$
$$\mathcal{S}^{1,NC}(\mathcal{T}) := \{V \in L^\infty(\Omega) : \ \forall T \in \mathcal{T}, \ V|_T \text{ affine } \wedge$$
$$\forall z \in \mathcal{M} \cap \Omega, \ V \text{ continuous at } z\},$$
$$\mathcal{S}^{1,NC}_0(\mathcal{T}) := \{V \in \mathcal{S}^{1,NC}(\mathcal{T}) : \ \forall z \in \mathcal{M} \setminus \Omega, \ V(z) = 0\}.$$

Define $\mathbf{f}_\mathcal{T} \in \mathcal{L}^0(\mathcal{T}|_\omega)$ by $\mathbf{f}_\mathcal{T}|_T = \int_T \mathbf{f} \, dx / |T|$, where $|T|$ denotes the area of $T \in \mathcal{T}$. The number of degrees of freedom $N = \dim(\mathcal{S}) + 2 \dim(\mathcal{L}^0(\mathcal{T}|_\omega))$ serves as a reference to the spatial discretisation $\mathcal{T}$, where $\mathcal{S} = \mathcal{S}^1_0(\mathcal{T})$ or $\mathcal{S}^{1,NC}_0(\mathcal{T})$.

The **Discrete Problem $(\mathbf{P}_N)$**:=$(\mathbf{P}|\mathcal{S}^1_0(\mathcal{T}) \times \mathcal{L}^0(\mathcal{T}|_\omega)^2 \times \mathcal{L}^0(\mathcal{T}|_\omega))$ for the conforming finite element method reads as follows: *Seek $(u_h, \mathbf{m}_h, \lambda_h)$ in $\mathcal{S}^1_0(\mathcal{T}) \times \mathcal{L}^0(\mathcal{T}|_\omega)^2 \times \mathcal{L}^0(\mathcal{T}|_\omega)$ satisfying*

$$(3.1) \qquad \int_\Omega \nabla u_h \cdot \nabla w_h \, dx = \int_\omega \mathbf{m}_h \cdot \nabla w_h \, dx \quad (w_h \in \mathcal{S}^1_0(\mathcal{T})),$$

$$(3.2) \qquad \nabla u_h + D\phi^{**}(\mathbf{m}_h) + \lambda_h \mathbf{m}_h = \mathbf{f}_\mathcal{T} \quad \text{a.e. in } \omega,$$

(3.3) $0 \le \lambda_h, \quad |\mathbf{m}_h| \le 1, \quad \text{and} \quad \lambda_h(1 - |\mathbf{m}_h|)_+ = 0 \quad$ a.e. in ω.

To describe the nonconforming finite element method, we define the $\mathcal{T}$-piecewise gradient $\nabla_\mathcal{T}$ by $\nabla_\mathcal{T} U(x) := \nabla U|_T(x)$ for $x \in T \in \mathcal{T}$, which may be different from the distributional gradient $\nabla U \in \mathcal{D}'(\Omega)$. Therefore, the discrete energy space is $H^1(\mathcal{T})$,

$$H^k(\mathcal{T}) := H^k(\bigcup_{T \in \mathcal{T}} \text{int}(T))$$

$$(3.4) \qquad := \{V \in L^2(\Omega) : \ \forall T \in \mathcal{T}, \ V|_T \in H^k(T)\}.$$

The **Discrete Problem** $(\mathbf{P}_N^{NC})$:=$(\mathbf{P}|\mathcal{S}_0^{1,NC}(\mathcal{T}) \times \mathcal{L}^0(\mathcal{T}|_\omega)^2 \times \mathcal{L}^0(\mathcal{T}|_\omega))$ for the nonconforming finite element method reads as follows: *Seek* $(u_h, \mathbf{m}_h, \lambda_h)$ *in* $\mathcal{S}_0^{1,NC}(\mathcal{T}) \times \mathcal{L}^0(\mathcal{T}|_\omega)^2 \times \mathcal{L}^0(\mathcal{T}|_\omega)$ *satisfying*

$$(3.5) \quad \int_\Omega \nabla_\mathcal{T} u_h \cdot \nabla_\mathcal{T} w_h \, dx = \int_\omega \mathbf{m}_h \cdot \nabla_\mathcal{T} w_h \, dx \quad (w_h \in \mathcal{S}_0^{1,NC}(\mathcal{T})),$$

$$(3.6) \qquad \nabla_\mathcal{T} u_h + D\phi^{**}(\mathbf{m}_h) + \lambda_h \mathbf{m}_h = \mathbf{f}_\mathcal{T} \quad \text{a.e. in } \omega,$$

$$(3.7) \ \ 0 \le \lambda_h, \quad |\mathbf{m}_h| \le 1, \quad \text{and} \quad \lambda_h(1 - |\mathbf{m}_h|)_+ = 0 \quad \text{a.e. in } \omega.$$

For a positive ε and the conforming resp. nonconforming discrete space $\mathcal{S}$, the **Discrete Penalised Problem** $(\mathbf{P}_\varepsilon|\mathcal{S} \times \mathcal{L}^0(\mathcal{T}|_\omega)^2 \times \mathcal{L}^0(\mathcal{T}|_\omega))$ abbreviated $(\mathbf{P}_{\varepsilon,N})$ for $\mathcal{S} = \mathcal{S}_0^1(\mathcal{T})$ resp. $(\mathbf{P}_{\varepsilon,N}^{NC})$ for $\mathcal{S} = \mathcal{S}_0^{1,NC}(\mathcal{T})$ reads as follows: *Seek* $(u_h, \mathbf{m}_h, \lambda_h)$ *in* $\mathcal{S} \times \mathcal{L}^0(\mathcal{T}|_\omega)^2 \times \mathcal{L}^0(\mathcal{T}|_\omega)$ *satisfying*

$$(3.8) \quad \int_\Omega \nabla_\mathcal{T} u_h \cdot \nabla_\mathcal{T} w_h \, dx = \int_\omega \mathbf{m}_h \cdot \nabla_\mathcal{T} w_h \, dx \quad (w_h \in \mathcal{S}),$$

$$(3.9) \qquad \nabla_\mathcal{T} u_h + D\phi^{**}(\mathbf{m}_h) + \lambda_h \mathbf{m}_h = \mathbf{f}_\mathcal{T} \quad \text{a.e. in } \omega,$$

$$(3.10) \qquad \lambda_h = \varepsilon^{-1}(|\mathbf{m}_h| - 1)_+/|\mathbf{m}_h| \quad \text{a.e. in } \omega.$$

Here, $(1 - |\mathbf{m}_h|)_+/|\mathbf{m}_h|$ is understood to vanish if $\mathbf{m}_h = 0$ (and $\nabla_\mathcal{T}$ could be replaced by ∇ in the conforming case $\mathcal{S} = \mathcal{S}_0^1(\mathcal{T})$).

The existence of discrete solutions follows as in the continuous case from the variational problem. Example 1.1, illustrated in Fig. 1, shows that $(\mathbf{P}_N)$ does allow multiple solutions for the uniaxial case in general while $(\mathbf{P}_N^{NC})$ does not.

Theorem 3.1. *In the uniaxial case, where $\phi^{**}(\mathbf{m}) = \frac{1}{2}(\mathbf{m} \cdot \mathbf{e}_\perp)^2$ for some unit vector $\mathbf{e} \in \mathbb{R}^2$ and its normal $\mathbf{e}_\perp$, Problems $(\mathbf{P}_N^{NC})$ and $(\mathbf{P}_{\varepsilon,N}^{NC})$ have unique solutions.*

Proof. Suppose $(u_j, \mathbf{m}_j, \lambda_j)$ solves $(\mathbf{P}_N^{NC})$ for $j = 1, 2$ and denote $e := u_2 - u_1 \in \mathcal{S}_0^{1,NC}(\mathcal{T})$ and $\boldsymbol{\delta} := \mathbf{m}_2 - \mathbf{m}_1 \in \mathcal{L}^0(\mathcal{T}|_\omega)^2$ (we neglect the lower index h in this proof for simplicity). According to (3.8), we have

$$(3.11) \qquad \int_\omega \nabla_\mathcal{T} e \cdot \boldsymbol{\delta} \, dx = \|\nabla_\mathcal{T} e\|_{2,\Omega}^2.$$

Subtracting the two equations in (3.9) for $j = 1, 2$ and multiplying the results with $\boldsymbol{\delta}$ we infer with (3.11) that

$$(3.12) \quad ||\nabla_{\mathcal{T}} e||^2_{2,\Omega} + \int_\omega (D\phi^{**}(\mathbf{m}_2) - D\phi^{**}(\mathbf{m}_1)) \cdot \boldsymbol{\delta} \, dx$$
$$+ \int_\omega (\lambda_2 \, \mathbf{m}_2 - \lambda_1 \, \mathbf{m}_1) \cdot \boldsymbol{\delta} \, dx = 0.$$

All the terms in (3.12) are non-negative and so will vanish separately. This follows for the second term in (3.12) from the convexity of ϕ^{**} (i.e., the monotonicity of $D\phi^{**}$) as we have $0 \leq (D\phi^{**}(b) - D\phi^{**}(a))(b - a)$ for all $a, b \in \mathbb{R}^2$. This is also true for the last term according to (3.10) and the elementary inequality

$$(3.13) \qquad 0 \leq ((|b| - 1)_+ b/|b| - (|a| - 1)_+ a/|a|) \cdot (b - a)$$

for all $a, b \in \mathbb{R}^2$. (To prove (3.13) we may assume in the first case $|a| \leq 1 < |b|$, where (3.13) is obvious, and in the remaining second case $1 < |a| \leq |b|$, where (3.13) follows from a straight forward calculation that shows that $(|b| - 1)(|b| - |a|) - (|a| - 1)(|b| - |a|) \geq 0$ is a lower bound of the right-hand side of (3.13).) Hence, (3.12) implies $\mathbf{e} = 0$ and $\boldsymbol{\delta} \cdot \mathbf{e}_\perp = 0$. A discrete Helmholtz decomposition of $\boldsymbol{\delta} \in L^2(\Omega)^2$ (extended by zero outside of ω) yields

$$(3.14) \qquad\qquad \boldsymbol{\delta} = \nabla_{\mathcal{T}} \alpha_h + \mathrm{curl}\, \beta_h \qquad \text{a.e. in } \Omega$$

for some $\alpha_h \in \mathcal{S}_0^{1,NC}(\mathcal{T})$ and $\beta_h \in \mathcal{S}^1(\mathcal{T})/\mathbb{R}$ [AF]. From (3.8) and $\mathbf{e} = 0$ (with $w_h = \alpha_h$) we deduce $\alpha_h = 0$ according to the L^2-orthogonality of $\nabla_{\mathcal{T}} \alpha_h$ and $\mathrm{curl}\, \beta_h$. With $\boldsymbol{\delta} = \mathrm{curl}\, \beta_h$ parallel to $\mathbf{e}$ we conclude that $\partial \beta_h / \partial \mathbf{e}_\perp = 0$ almost everywhere in Ω. Note that $\boldsymbol{\delta} = 0$ and so $\nabla \beta_h = 0$ on $\Omega \setminus \omega$. Hence, β_h is constant on the connected open set $\Omega \setminus \overline{\omega}$, without loss of generality, $\beta_h = 0$ on $\Omega \setminus \overline{\omega}$. Integrating along lines parallel to $\mathbf{e}_\perp$ we deduce that $\beta_h = 0$ almost everywhere on Ω and so $\boldsymbol{\delta} = 0$. The proof is finished for $(\mathrm{P}_{\varepsilon,N}^{NC})$.

The proof of uniqueness for solutions of (P_N^{NC}) is analogous except that the non-negativeness of the last term in (3.12) is verified with the monotone relation in (3.7). An elementary analysis with $\lambda_1 \leq \lambda_2$ reveals $0 \leq (\lambda_2 \, \mathbf{m}_2 - \lambda_1 \, \mathbf{m}_1) \cdot (\mathbf{m}_2 - \mathbf{m}_1)$ pointwise almost everywhere. The remaining details are omitted. $\qquad\qquad\qquad\qquad\qquad\qquad\qquad\qquad\qquad\qquad\qquad\qquad$ □

This section is concluded with an example which shows that, in general, the magnetisation is *not* necessarily convergent in $L^2(\omega)^2$. As a consequence, we must not expect to prove error estimates for $\mathbf{m} - \mathbf{m}_h$ in the L^2-norm and have to analyse which quantities can be estimated in the following sections.

Example 3.1. Suppose $\mathcal{T}|_\omega = \{T_1, T_2, \ldots, T_{2J}\}$ is a structured triangulation of ω which consists of halved squares $Q_j = T_{2j-1} \cup T_{2j}, j = 1, \ldots, J,$ as in Example 1.1 with a diagonal parallel to the easy axis $\mathbf{e} = (1,1)/\sqrt{2}$ in the uniaxial case (cf. Fig. 1). Suppose $(u, \mathbf{m}, \lambda)$ solves (1.1)-(1.2) while $(u_h, \mathbf{m}_h, \lambda_h)$ is a solution to (P_N) or $(P_{\varepsilon,N})$. Then,

$$\sum_{j=1}^J \min\{\| 1 - |\mathbf{m}| \|_{L^2(T_{2j-1})}^2, \| 1 - |\mathbf{m}| \|_{L^2(T_{2j})}^2\}$$

$$\text{(3.15)} \qquad \leq 4 \max_{(u_h, \tilde{\mathbf{m}}_h, \lambda_h)} \| \mathbf{m} - \tilde{\mathbf{m}}_h \|_{L^2(\omega)}^2,$$

where $(u_h, \tilde{\mathbf{m}}_h, \lambda_h)$ denotes an arbitrary solution to (P_N) or $(P_{\varepsilon,N})$. Note that the left-hand side of (3.15) is uniformly positive (for a mesh-size tending to zero) if, for instance, the set $\{x \in \omega : |\mathbf{m}(x)| < 1 - \delta\}$ has no interior point for all $0 < \delta < 1$.

Proof of (3.15). Let $\mu_j := \max\{|\mathbf{m}_h|_{T_{2j-1}}, |\mathbf{m}_h|_{T_{2j}}\}$ and suppose without loss of generality that $\mu_j = |\mathbf{m}_h|_{T_{2j}}$ for all $j = 1, \ldots, J$. Set $\mathbf{m}_h \in \mathcal{L}^0(\mathcal{T})$ with $M_h|_{T_{2j-2+k}} := (1 - \mu_j)_+ (-1)^k (1,1)/\sqrt{2}$ for $j = 1, \ldots, J,$ $k = 1, 2$. Arguing as in Example 1.1, we observe that $(u_h, \mathbf{m}_h \pm \mathbf{M}_h, \lambda_h)$ is also a discrete solution. A triangle inequality shows

(3.16)
$$\| M_h \|_{2,\omega} \leq \frac{1}{2}\| \mathbf{m} - \mathbf{m}_h + \mathbf{M}_h \|_{2,\omega} + \frac{1}{2}\| \mathbf{m} - \mathbf{m}_h - \mathbf{M}_h \|_{2,\omega} \leq M,$$

where M denotes the right-hand side of (3.15). Young's inequality is applied to $0 \leq 1 - |\mathbf{m}| \leq 1 - |\mathbf{m}_h| + |\mathbf{m} - \mathbf{m}_h|$ and shows

$$\frac{1}{2}\sum_{j=1}^J \| 1 - |\mathbf{m}| \|_{2,T_{2j}}^2 \leq \sum_{j=1}^J \| 1 - |\mathbf{m}_h| \|_{2,T_{2j}}^2 + \sum_{j=1}^J \| \mathbf{m} - \mathbf{m}_h \|_{2,T_{2j}}^2$$

$$\text{(3.17)} \qquad \leq M^2 + \sum_{j=1}^J \| \mathbf{M}_h \|_{2,T_{2j}}^2 \leq 2 M^2$$

because of the definition of $\mathbf{M}_h$ and (3.16). □

Remark 3.1. This understanding of instable and stable numerical schemes for problem (M_0) might lead to some rigorous insight in the resonance of instable numerical schemes with oscillating microstructures for problem (M_α).

4. A priori error estimates

To describe the a priori error estimates in the conforming discrete model
$(P_{\varepsilon,N})$, let $(\cdot)_{\mathcal{T}}$ denote the $\mathcal{T}$-piecewise integral means such as $\mathbf{m}_{\mathcal{T}} \in$
$\mathcal{L}^0(\mathcal{T}|_\omega)$ given by

$$(4.1) \qquad \mathbf{m}_{\mathcal{T}}|_T = \int_T \mathbf{m}\, dx/|T| \qquad (T \in \mathcal{T}_\omega)$$

and let $P_1 : H_0^1(\Omega) \to \mathcal{S}_1(\mathcal{T})$ denote the Galerkin projector.

Theorem 4.1. *Suppose $(u, \mathbf{m}, \lambda)$ solves Problem (P) and $(u_h, \mathbf{m}_h, \lambda_h)$
solves the Discrete Problem $(P_{\varepsilon,N})$. Then we have*

$$\frac{1}{2}\|\nabla(u - u_h)\|_{L^2(\Omega)}^2 + \frac{1}{2}\int_\omega \varepsilon\lambda_h^2|\mathbf{m}_h|^2 dx$$

$$+ \int_\omega (D\phi^{**}(\mathbf{m}) - D\phi^{**}(\mathbf{m}_h)) \cdot (\mathbf{m} - \mathbf{m}_h) dx$$

$$\leq \frac{1}{2}\int_\omega \varepsilon\lambda^2 dx + \frac{1}{2}\|\mathbf{f} - \mathbf{f}_{\mathcal{T}}\|_{L^2(\omega)}^2 + \frac{1}{2}\|\mathbf{m} - \mathbf{m}_{\mathcal{T}}\|_{L^2(\omega)}^2$$

$$(4.2) \qquad + \|\nabla(u - P_1 u)\|_{L^2(\Omega)}^2 + \|\mathbf{m} - \mathbf{m}_h\|_{2,\omega}\|\nabla(u - P_1 u)\|_{L^2(\Omega)}.$$

To establish convergence of the discrete function $\lambda_h \mathbf{m}_h$ towards $\lambda\mathbf{m}$,
we suppose that $\phi^{\star\star}$ satisfies, for all $\mathbf{m}_1, \mathbf{m}_2 \in \mathbb{R}^2$,

$$c_1|D\phi^{\star\star}(\mathbf{m}_2) - D\phi^{\star\star}(\mathbf{m}_1)|^2$$
$$(4.3) \qquad \leq \big((D\phi^{\star\star}(\mathbf{m}_2) - D\phi^{\star\star}(\mathbf{m}_1)) \cdot (\mathbf{m}_2 - \mathbf{m}_1)\big)$$

for some constant $c_1 > 0$. Note that this covers the uniaxial case with $c_1 = 1$.
Let $(\lambda\mathbf{m})_{\mathcal{T}} \in \mathcal{L}^0(\mathcal{T})$ denote the $\mathcal{T}$-piecewise integral mean of $\lambda\mathbf{m}$.

Theorem 4.2. *Suppose that ϕ^{**} satisfies (4.3) and that $(u, \mathbf{m}, \lambda)$ solves
Problem (P) and $(u_h, \mathbf{m}_h, \lambda_h)$ solves the Discrete Problem $(P_{\varepsilon,N})$. Then,
there exists an $h_{\mathcal{T}}$-independent constant $c_2 > 0$ such that*

$$\|\nabla(u - u_h)\|_{L^2(\Omega)}^2 + \|D\phi^{\star\star}(\mathbf{m}) - D\phi^{\star\star}(\mathbf{m}_h)\|_{L^2(\omega)}^2$$

$$+ \|\lambda\mathbf{m} - \lambda_h\mathbf{m}_h\|_{L^2(\omega)}^2$$

$$\leq c_2\Big(\|\varepsilon\lambda\|_{L^2(\omega)}^2 + \|\mathbf{f} - \mathbf{f}_{\mathcal{T}}\|_{2,\omega}^2 + \|\mathbf{m} - \mathbf{m}_{\mathcal{T}}\|_{2,\omega}^2$$

$$+ \|\lambda\mathbf{m} - (\lambda\mathbf{m})_{\mathcal{T}}\|_{L^2(\omega)}^2 + \|\nabla(u - P_1 u)\|_{2,\Omega}^2$$

$$(4.4) \qquad + \|\mathbf{m} - \mathbf{m}_h\|_{2,\omega}\|\nabla(u - P_1 u)\|_{2,\Omega}\Big).$$

*The constant c_2 depends on c_1 and the shape of the elements but neither on
their sizes $h_{\mathcal{T}}$ nor on $\mathbf{f}, \mathbf{m}, u, \lambda, \Omega, \omega, \mathbf{m}_h, u_h$, or λ_h.*

Remarks 4.1. (i) Since ϕ^{**} is convex, $0 \leq (D\phi^{**}(\mathbf{m}) - D\phi^{**}(\mathbf{M})) \cdot (\mathbf{m} - \mathbf{M})$ for all $\mathbf{m}, \mathbf{M} \in \mathbb{R}^2$ and so $(D\phi^{**}(\mathbf{m}) - D\phi^{**}(\mathbf{m}_h)) \cdot (\mathbf{m} - \mathbf{m}_h)$ is non-negative pointwise almost everywhere. Hence, the lower bound in (4.8) consists of non-negative summands. For the uniaxial case where $\phi^{**}(\mathbf{m}) = \frac{1}{2}(\mathbf{m} \cdot \mathbf{e}_\perp)^2$,

(4.5)
$$\int_\omega (D\phi^{**}(\mathbf{m}) - D\phi^{**}(\mathbf{m}_h)) \cdot (\mathbf{m} - \mathbf{m}_h)dx = \| (\mathbf{m} - \mathbf{m}_h) \cdot \mathbf{e}_\perp \|_2^2$$

all the theorems in this section yield estimates for the L^2-norm of the $\mathbf{e}_\perp$-component of the error in the magnetisation.
(ii) In case of multiple exact or discrete solutions, any selection of a pair of them is considered in the theorems.
(iii) Under sufficient regularity of the exact solution, the above theorems provide the estimate

(4.6) $\quad \| \nabla(u - u_h) \|_{L^2(\Omega)} + \| (\mathbf{m} - \mathbf{m}_h) \cdot \mathbf{e}_\perp \|_{L^2(\omega)} = \mathcal{O}(\varepsilon + \sqrt{h})$

in the uniaxial case and the conforming scheme.
(iv) The last term in (4.2) is the limiting quantity in the upper bound and causes the result to be suboptimal, in general. In fact, the term $\| \mathbf{m} - \mathbf{m}_h \|_{2,\omega}$ can only be controlled by the Lebesgue measure of the domain ω plus higher order terms (cf. Example 3.1).
(v) The generic convergence order in (4.6) suggests the choice $\varepsilon = \mathcal{O}(\sqrt{h})$. Numerical evidence in the examples of Sect. 7 convinced us to prefer $\varepsilon = \mathcal{O}(h)$.

To describe our result for the nonconforming scheme, let $I_\mathcal{T}u \in \mathcal{S}_0^{1,NC}(\mathcal{T})$ denote the interpolation for the Crouzeix-Raviart finite element defined by

(4.7) $\qquad I_\mathcal{T}u(z) = h_E^{-1} \int_E u \, ds \qquad (z \in E \cap \mathcal{M},\ E \in \mathcal{E})$

for any $u \in H_0^1(\Omega)$. The weight $h_\mathcal{T} \in \mathcal{L}^0(\mathcal{T})$ represents the local mesh-size, $h_\mathcal{T}|_T = h_T := \mathrm{diam}(T)$ for $T \in \mathcal{T}$.

Theorem 4.3. *Suppose $(u, \mathbf{m}, \lambda)$ solves Problem (P) and $(u_h, \mathbf{m}_h, \lambda_h)$ solves the Discrete Penalised Problem $(P_{\varepsilon,N}^{NC})$. Then, there exists an $h_\mathcal{T}$-independent constant $c_3 > 0$ such that*

$$\frac{1}{2}\| \nabla_\mathcal{T}(u - u_h) \|_{L^2(\Omega)}^2 + \frac{1}{2}\int_\omega \varepsilon\lambda_h^2|\mathbf{m}_h|^2 dx$$

$$+ \int_\omega (D\phi^{**}(\mathbf{m}) - D\phi^{**}(\mathbf{m}_h)) \cdot (\mathbf{m} - \mathbf{m}_h)dx$$

$$\leq \frac{1}{2} \int_\omega \varepsilon \lambda^2 dx + \frac{1}{2} \| \mathbf{f} - \mathbf{f}_\mathcal{T} \|^2_{L^2(\omega)} + \| \mathbf{m} - \mathbf{m}_\mathcal{T} \|^2_{L^2(\omega)}$$

(4.8) $$+ \frac{3}{2} \| \nabla_\mathcal{T}(u - I_\mathcal{T} u) \|^2_{L^2(\Omega)} + c_3 \| h_\mathcal{T} \nabla_\mathcal{T}(\mathbf{m} - \nabla u) \|^2_{L^2(\Omega)}.$$

The constant c_3 depends only on the shape on the elements but neither on their sizes nor on $\mathbf{f}, \mathbf{m}, u, \lambda, \Omega, \omega, \mathbf{m}_h, u_h$, or λ_h.

Theorem 4.4. *Suppose that ϕ^{**} satisfies (4.3) and that $(u, \mathbf{m}, \lambda)$ solves Problem (P) and $(u_h, \mathbf{m}_h, \lambda_h)$ solves the Discrete Problem $(P^{NC}_{\varepsilon,N})$. Then, there exists an $h_\mathcal{T}$-independent constant $c_4 > 0$ such that*

$$\int_\Omega |\nabla_\mathcal{T}(u - u_h)|^2 \, dx$$

$$+ \int_\omega |D\phi^{**}(\mathbf{m}) - D\phi^{**}(\mathbf{m}_h)|^2 dx + \int_\omega |\lambda \mathbf{m} - \lambda_h \mathbf{m}_h|^2 dx$$

$$\leq c_4 \Big(\int_\omega \varepsilon^2 \lambda^2 dx + \| \mathbf{f} - \mathbf{f}_\mathcal{T} \|^2_{2,\omega} + \| \mathbf{m} - \mathbf{m}_\mathcal{T} \|^2_{L^2(\omega)}$$

$$+ \| \nabla_\mathcal{T}(u - I_\mathcal{T} u) \|^2_{2,\Omega} + \| h_\mathcal{T} \nabla_\mathcal{T}(\mathbf{m} - \nabla_\mathcal{T} u) \|^2_{L^2(\Omega)}$$

(4.9) $$+ \| \lambda \mathbf{m} - (\lambda \mathbf{m})_\mathcal{T} \|^2_{L^2(\omega)} \Big).$$

The constant c_4 depends on c_1 and the shape of the elements but neither on their sizes $h_\mathcal{T}$ nor on $f, \mathbf{m}, u, \lambda, \Omega, \omega, \mathbf{m}_h, u_h$, or λ_h.

Remarks 4.2. (i) Under sufficient regularity of the exact solution, the above two theorems provide the estimate

(4.10) $$\| \nabla_\mathcal{T}(u - u_h) \|_{L^2(\Omega)} + \| (\mathbf{m} - \mathbf{m}_h) \cdot \mathbf{e}_\perp \|_{L^2(\omega)} = \mathcal{O}(\varepsilon + h)$$

in the uniaxial case and the nonconforming scheme.
(ii) The generic convergence order $O(\epsilon + h)$ suggests the choice $\varepsilon = \mathcal{O}(h)$ in agreement with numerical experience reported in Sect. 7 below.
(iii) The proof of Theorem 4.3 reveals that $\int_\omega \varepsilon \lambda^2 dx$ on the right-hand side of (4.8) could be replaced by the smaller contribution $\int_{\omega_h} \varepsilon \lambda^2 dx$ on the smaller domain $\omega_h := \{x \in \omega : \lambda_h(x) > 0\}$. This observation will affect the a posteriori error estimates of Sect. 5.

The remaining part of this section is devoted to the proofs the four theorems of this section.

Proof of Theorem 4.3. In the first part of the proof, the convexity of the indicator function ψ and the penalisation in (3.10) yield the estimate

(4.11) $$\frac{\varepsilon}{2} |\mathbf{m}_h|^2 \lambda_h^2 \leq (\lambda \mathbf{m} - \lambda_h \mathbf{m}_h) \cdot (\mathbf{m} - \mathbf{m}_h) + \frac{\varepsilon}{2} \lambda^2.$$

Indeed, direct calculations which merely involve $|\mathbf{m}| \leq 1$ and Cauchy's inequality reveal

$$(4.12) \qquad -\lambda \mathbf{m} \cdot (\mathbf{m} - \mathbf{m}_h) \leq \lambda(|\mathbf{m}_h| - 1) = \varepsilon \lambda \lambda_h |\mathbf{m}_h|,$$

$$(4.13) \qquad \varepsilon \lambda_h^2 |\mathbf{m}_h|^2 \leq \lambda_h \mathbf{m}_h \cdot (\mathbf{m}_h - \mathbf{m}).$$

Adding (4.12) and (4.13) we obtain (4.11) with Young's inequality, $\lambda \lambda_h \varepsilon |\mathbf{m}_h| \leq \frac{\varepsilon}{2} \lambda^2 + \frac{\varepsilon}{2} |\mathbf{m}_h|^2 \lambda_h^2$.

In the second step we provide the identity

$$(4.14) \qquad \int_\omega (\mathbf{m}_h - \mathbf{m}_\mathcal{T}) \cdot \nabla_\mathcal{T}(u - I_\mathcal{T}u) dx = 0$$

which follows elementwise from (4.7): An integration by parts gives

$$
\begin{aligned}
(4.15) \qquad \int_T \nabla_\mathcal{T}(u - I_\mathcal{T}u) dx &= \int_{\partial T} (u - I_\mathcal{T}u) n \, ds \\
&= \sum_{E \in \mathcal{E}} n_E \int_{E \cap \partial T} (u - I_\mathcal{T}u) \, ds = 0
\end{aligned}
$$

since the normal vector n_E on the edge $E \in \mathcal{E}$ is constant. Because $\mathbf{m}_h - \mathbf{m}_\mathcal{T} \in \mathcal{L}^0(\mathcal{T}|_\omega)$, (4.15) proves (4.14).

For the remaining part of the proof, we abbreviate $e := u - u_h$, $\boldsymbol{\delta} := \mathbf{m} - \mathbf{m}_h$ and let $w_h := -u_h + I_\mathcal{T}u \in \mathcal{S}_0^{1,NC}(\mathcal{T})$. In step three we perform a standard calculation [BS] for non-conforming finite elements. The Galerkin-orthogonality for (2.5) and (3.8) leads to

$$
\begin{aligned}
(4.16) \\
\int_\Omega \nabla_\mathcal{T}e \cdot \nabla_\mathcal{T}w_h \, dx - \int_\omega \boldsymbol{\delta} \cdot \nabla_\mathcal{T}w_h \, dx = \int_{\cup\mathcal{E}} (\nabla u - \mathbf{m}) \cdot n_E \, [w_h] \, ds,
\end{aligned}
$$

where $[w_h]$ denotes the jump of w_h along the edge $E \in \mathcal{E}$ with normal vector n_E and $\mathbf{m} = 0$ outside of ω.

In step four, we consider the difference of (2.6) and (3.9) and multiply with $\boldsymbol{\delta}$ to obtain finally that

$$
\begin{aligned}
(4.17) \qquad \int_\omega \boldsymbol{\delta} \cdot \nabla_\mathcal{T}e \, dx &= \int_\omega (\mathbf{m} - \mathbf{m}_\mathcal{T}) \cdot (\mathbf{f} - \mathbf{f}_\mathcal{T}) dx \\
&\quad - \int_\omega (D\phi^{**}(\mathbf{m}) - D\phi^{**}(\mathbf{m}_h)) \cdot \boldsymbol{\delta} \, dx \\
&\quad - \int_\omega (\lambda\mathbf{m} - \lambda_h\mathbf{m}_h) \cdot \boldsymbol{\delta} \, dx
\end{aligned}
$$

(notice $\int_T (\mathbf{m}_h - \mathbf{m}_\mathcal{T}) \cdot (\mathbf{f} - \mathbf{f}_\mathcal{T}) dx = 0$).

In the final step we collect the preceding estimates. Rewriting (4.17) with adding $\| \nabla_{\mathcal{T}} e \|_{2,\Omega}^2$ and then employing (4.16) we obtain with Cauchy's and Young's inequalities

$$\int_\omega (D\phi^{**}(\mathbf{m}) - D\phi^{**}(\mathbf{m}_h)) \cdot \boldsymbol{\delta} \, dx + \int_\omega (\lambda \mathbf{m} - \lambda_h \mathbf{m}_h) \cdot \boldsymbol{\delta} \, dx$$

$$+ \| \nabla_{\mathcal{T}} e \|_{2,\Omega}^2 - \frac{1}{2} \| \mathbf{m} - \mathbf{m}_{\mathcal{T}} \|_{2,\Omega}^2 - \frac{1}{2} \| \mathbf{f} - \mathbf{f}_{\mathcal{T}} \|_{2,\Omega}^2$$

$$\leq \int_\Omega \nabla_{\mathcal{T}} e \cdot (\nabla_{\mathcal{T}} e - \boldsymbol{\delta}) dx$$

$$= \int_{\cup \mathcal{E}} (\nabla u - \mathbf{m}) \cdot n_E \, [I_{\mathcal{T}} u - u_h] \, ds$$

(4.18) $$+ \int_\Omega \nabla_{\mathcal{T}} (u - I_{\mathcal{T}} u) \cdot (\nabla_{\mathcal{T}} e - \boldsymbol{\delta}) dx.$$

According to (4.14), the last contribution of the right-hand side in (4.18) equals

(4.19) $$\int_\Omega \nabla_{\mathcal{T}} (u - I_{\mathcal{T}} u) \cdot \nabla_{\mathcal{T}} e \, dx - \int_\omega \nabla_{\mathcal{T}} (u - I_{\mathcal{T}} u) \cdot (\mathbf{m} - \mathbf{m}_{\mathcal{T}}) dx$$

$$\leq \| \nabla_{\mathcal{T}} e \|_{2,\Omega} \| u - I_{\mathcal{T}} u \|_{2,\Omega} + \| u - I_{\mathcal{T}} u \|_{2,\omega} \| \mathbf{m} - \mathbf{m}_{\mathcal{T}} \|_{2,\omega}.$$

A standard argument for the jumps $[I_{\mathcal{T}} u - u_h]$ with $\mathcal{E}$-piecewise integral mean zero shows

$$\int_{\cup \mathcal{E}} (\nabla u - \mathbf{m}) \cdot n_E \, [I_{\mathcal{T}} u - u_h] \, ds$$

(4.20) $$\leq \sqrt{c_3} \| h_{\mathcal{T}} \nabla_{\mathcal{T}} (\nabla u - \mathbf{m}) \|_{2,\Omega} \| \nabla_{\mathcal{T}} e \|_{2,\Omega}$$

with an $h_{\mathcal{T}}$-independent constant $c_3 > 0$ (which only depends on the shapes of the elements) [BS]. Using this in (4.18) and owing to (4.11), we finally deduce (4.8) by absorbing the error terms on the right-hand side. $\qquad \square$

Proof of Theorem 4.4. Let $(\lambda \mathbf{m})_{\mathcal{T}} \in \mathcal{L}^0(\mathcal{T}|_\omega)$ be defined by $(\lambda \mathbf{m})_{\mathcal{T}}|_T = \int_T \lambda \mathbf{m} \, dx / |T|$ for $T \in \mathcal{T}$. Set

$$A := \| \nabla_{\mathcal{T}} (u - u_h) \|_{2,\Omega} + \| D\phi^{**}(\mathbf{m}) - D\phi^{**}(\mathbf{m}_h) \|_{2,\omega}$$

$$+ \| \lambda \mathbf{m} - (\lambda \mathbf{m})_{\mathcal{T}} \|_{2,\omega},$$

$$B := \| \mathbf{f} - \mathbf{f}_{\mathcal{T}} \|_{2,\omega} + \| \mathbf{m} - \mathbf{m}_{\mathcal{T}} \|_{2,\omega} + \| \lambda \mathbf{m} - (\lambda \mathbf{m})_{\mathcal{T}} \|_{2,\omega}$$

$$+ \| \nabla_{\mathcal{T}} (u - I_{\mathcal{T}} u) \|_{2,\Omega} + \| h_{\mathcal{T}} \nabla_{\mathcal{T}} (\boldsymbol{\delta} - \nabla_{\mathcal{T}} u) \|_{2,\Omega}.$$

Subtract (3.6) from (2.6) and test with the admissible function $(\lambda \mathbf{m})_{\mathcal{T}} - \lambda_h \mathbf{m}_h$ to infer

(4.21) $$\| \lambda \mathbf{m} - \lambda_h \mathbf{m}_h \|_{2,\omega} \leq A + \| \mathbf{f} - \mathbf{f}_{\mathcal{T}} \|_{2,\omega} + \| \lambda \mathbf{m} - (\lambda \mathbf{m})_{\mathcal{T}} \|_{2,\omega}$$

$$\leq \frac{c_4}{2} \Big(B + \big(\int_\omega \varepsilon \lambda^2 \, dx \big)^{1/2} \Big).$$

Because of

$$\lambda_h^2|\mathbf{m}_h|^2 - \lambda^2|\mathbf{m}|^2 = \left(\lambda_h|\mathbf{m}_h| + \lambda|\mathbf{m}|\right)\left(\lambda_h|\mathbf{m}_h| - \lambda|\mathbf{m}|\right)$$

(4.22)
$$\leq \left(\lambda_h|\mathbf{m}_h| + \lambda|\mathbf{m}|\right)\left|\lambda_h\mathbf{m}_h - \lambda\mathbf{m}\right|$$

and Cauchy's inequality, we can conclude from (4.21) that

$$\left|\int_\omega \left(\lambda_h^2|\mathbf{m}_h|^2 - \lambda^2|\mathbf{m}|^2\right)dx\right| \leq \left(2\int_\omega \left(\lambda_h^2|\mathbf{m}_h|^2 + \lambda^2|\mathbf{m}|^2\right)dx\right)^{1/2}$$

$$\times\left(\int_\omega |\lambda_h\mathbf{m}_h - \lambda\mathbf{m}|^2 dx\right)^{1/2}$$

(4.23)
$$\leq c_4 c_5 A\left(\int_\omega \lambda^2 dx + B^2\right)^{1/2}.$$

Multiply (4.23) with $\varepsilon/2$ and recast it into

$$\frac{1}{2}\int_\omega \varepsilon\lambda^2|\mathbf{m}|^2\, dx \leq \frac{1}{2}\int_\omega \varepsilon\lambda_h^2|\mathbf{m}_h|^2\, dx$$

(4.24)
$$+\frac{c_6}{2} A\left(\int_\omega \varepsilon^2\lambda^2|\mathbf{m}|^2\, dx + \varepsilon^2 B^2\right)^{1/2}.$$

Adding this to (4.8) and employing (4.3) we conclude the proof of (4.9) by absorbing the first and second contribution in A.   □

Proof of Theorem 4.1.   The arguments in the proof of Theorem 4.4 apply to the conforming situation as well and jumps disappear (e.g., in (4.16), (4.18)). From (3.5) we obtain

(4.25) $$\int_\Omega \nabla e \cdot (\nabla e - \boldsymbol{\delta})dx = \int_\Omega \nabla(u - P_1 u) \cdot (\nabla e - \boldsymbol{\delta})dx,$$

using the Ritz-Galerkin projection P_1. Note that (4.14) is no longer available and so we end up with

$$\int_\Omega \nabla e \cdot (\nabla e - \boldsymbol{\delta})dx$$

(4.26) $$\leq \|\nabla(u - P_1 u)\|_{2,\Omega}\left(\|\boldsymbol{\delta}\|_{2,\omega} + \|\nabla(u - P_1 u)\|_{2,\Omega}\right).$$ □

Proof of Theorem 4.2.   Following the proof of Theorem 4.1 with the modification

(4.27) $$B := \|\mathbf{f} - \mathbf{f}_{\mathcal{T}}\|_{2,\omega} + \|\mathbf{m} - \mathbf{m}_{\mathcal{T}}\|_{2,\omega} + \|\lambda\mathbf{m} - (\lambda\mathbf{m})_{\mathcal{T}}\|_{2,\omega}$$

$$+ \|\nabla(u - P_1 u)\|_{2,\Omega}\|\mathbf{m} - \mathbf{m}_{\mathcal{T}}\|_{2,\omega}^{1/2}\|\nabla(u - P_1 u)\|_{2,\Omega}^{1/2}$$

we verify Theorem 4.2.   □

5. Reliable or efficient a posteriori error estimates

The a posteriori error estimates differ essentially for conforming and non-conforming schemes. First, our results are stated, then discussed and proved at the end of this section. Numerical tests on adaptive algorithms for automatic mesh-refining will be reported on in the subsequent section.

The discrete function $\mathbf{m}_h - \nabla u_h$ is $\mathcal{T}$-piecewise constant and its jump across an interior edge $E \in \mathcal{E}$ with a chosen unit normal vector n_E and length h_E is written $[\mathbf{m}_h - \nabla u_h] \cdot n_E$. We abbreviate the $\mathcal{E}$-piecewise constant edge-size and the chosen normal n_E on the skeleton $\cup \mathcal{E} = \cup_{T \in \mathcal{T}} \partial T$ (the union of all points which belong to an edge) by $h_\mathcal{E} \in L^\infty(\cup \mathcal{E})$ and $n_\mathcal{E} \in L^\infty(\cup \mathcal{E})^2$ defined by $(h_\mathcal{E})|_E := h_E := \operatorname{diam}(E)$ and $(n_\mathcal{E})|_E := n_E$ for $E \in \mathcal{E}$ in Ω. On the outer boundary we formally set $(n_\mathcal{E})|_{\partial \Omega} = 0$ such that all terms disappear there. A crucial role plays the sub-domain ω_h of ω where λ_h is positive,

$$(5.1) \qquad\qquad \omega_h = \{x \in \omega : 0 < \lambda_h(x)\}.$$

Theorem 5.1. *Suppose that ϕ^{**} satisfies (4.3), $0 < \varepsilon < \min\{1, c_1\}$, and that $(u, \mathbf{m}, \lambda)$ solves Problem (P) and $(u_h, \mathbf{m}_h, \lambda_h)$ solves the Discrete Problem ($P_{\varepsilon,N}$). Then there exists an $(\varepsilon, h_\mathcal{T}, h_\mathcal{E})$-independent constant c_7 with*

$$\| \nabla(u - u_h) \|_{L^2(\Omega)}^2 + c_1 \| D\phi^{**}(\mathbf{m}) - D\phi^{**}(\mathbf{m}_h) \|_{L^2(\omega)}^2$$

$$\leq (3 + 1/c_1) \| \varepsilon \lambda_h \mathbf{m}_h \|_{L^2(\omega_h)}^2 + \int_\omega (\mathbf{m} - \mathbf{m}_\mathcal{T}) \cdot (\mathbf{f} - \mathbf{f}_\mathcal{T}) \, dx$$

$$(5.2) \qquad + \| \mathbf{f} - \mathbf{f}_\mathcal{T} \|_{L^2(\omega_h)}^2 + c_7^2 \| h_\mathcal{E}^{1/2} [\mathbf{m}_h - \nabla u_h] \cdot n_\mathcal{E} \|_{L^2(2, \cup \mathcal{E})}^2.$$

The constant c_7 depends on the shape of the elements in $\mathcal{T}$ but neither on their sizes nor on the data $\mathbf{f}$ or solutions $u, \mathbf{m}, \lambda, u_h, \mathbf{m}_h, \lambda_h$.

The situation is more involved for nonconforming schemes. The nonconformity is controlled by an edge term $[\partial u_h / \partial s]$, where $\partial / \partial s$ denotes the derivative with respect to the arc-length along $E \in \mathcal{E}$ and $[\partial u_h / \partial s]$ is the jump across E of $\partial u_h / \partial s$ from either sides. We regard $[\partial u_h / \partial s]$ as a function on $\cup \mathcal{E}$ which is $-\partial u_h / \partial s$ on $\partial \Omega$.

Theorem 5.2. *Suppose that ϕ^{**} satisfies (4.3), $0 < \varepsilon < \min\{1, c_1\}$, and that Ω is simply connected. Let $(u, \mathbf{m}, \lambda)$ solve Problem (P) and let $(u_h, \mathbf{m}_h, \lambda_h)$ solve the Penalised Discrete Problem ($P_{\varepsilon,N}^{NC}$). Then there exists an $(\varepsilon, h_\mathcal{T}, h_\mathcal{E})$-independent constant c_8 with*

$$\| \nabla_\mathcal{T}(u - u_h) \|_{L^2(\Omega)}^2 + c_1 \| D\phi^{**}(\mathbf{m}) - D\phi^{**}(\mathbf{m}_h) \|_{2,\omega}^2$$

$$\leq (2 + 1/c_1) \| \varepsilon \lambda_h \mathbf{m}_h \|_{L^2(\omega_h)}^2 + \| \mathbf{f} - \mathbf{f}_\mathcal{T} \|_{L^2(\omega_h)}^2$$

$$(5.3) \qquad +2 \int_\omega (\mathbf{m} - \mathbf{m}_\mathcal{T}) \cdot (\mathbf{f} - \mathbf{f}_\mathcal{T}) \, dx + c_8^2 \| \, h_\mathcal{E}^{1/2} [\partial u_h / \partial s] \, \|_{L^2(\cup \mathcal{E})}.$$

The constant c_8 depends on the shape of the elements in $\mathcal{T}$ but neither on their sizes nor on the data f or solutions $u, \mathbf{m}, \lambda, u_h, \mathbf{m}_h, \lambda_h$.

In case that the exact solution is smooth, i.e., $\mathbf{m} - \nabla u|_\omega \in W^{1,\infty}(\omega)^2$, we have

$$\| \nabla_\mathcal{T}(u - u_h) \|_{L^2(\Omega)}^2 + c_1 \| \, D\phi^{**}(\mathbf{m}) - D\phi^{**}(\mathbf{m}_h) \, \|_{2,\omega}^2$$

$$\leq (2 + 1/c_1) \| \, \varepsilon \lambda_h \mathbf{m}_h \, \|_{L^2(\omega_h)}^2 + \| \, \mathbf{f} - \mathbf{f}_\mathcal{T} \, \|_{L^2(\omega_h)}^2$$

$$(5.4) \qquad +2 \int_\omega (\mathbf{m} - \mathbf{m}_\mathcal{T}) \cdot (\mathbf{f} - \mathbf{f}_\mathcal{T}) \, dx + c_9^2 \| \, h_\mathcal{E}^2 [\partial u_h / \partial s] \, \|_{L^1(\cup \mathcal{E})}$$

for an $(\varepsilon, h_\mathcal{T}, h_\mathcal{E})$-independent constant $c_9 > 0$ which depends on $| \, \mathbf{m} - \nabla u|_\omega \, |_{W^{1,\infty}(\omega)}$.

Remarks 5.1. (i) Note that $|\mathbf{m}| \leq 1$ pointwise almost everywhere in Ω implies $\| \, \mathbf{m} - \mathbf{m}_\mathcal{T} \, \|_{L^\infty(\omega)} \leq 2$ and so, the first term on the right-hand side of (5.8) is estimated by

$$(5.5) \qquad \int_\omega (\mathbf{m} - \mathbf{m}_\mathcal{T}) \cdot (\mathbf{f} - \mathbf{f}_\mathcal{T}) \, dx \leq 2 \, \| \, \mathbf{f} - \mathbf{f}_\mathcal{T} \, \|_{L^1(\Omega)}.$$

In case $\mathbf{m} \in W^{1,\infty}(\omega)^2$, a Poincaré type estimate shows

$$(5.6) \quad \int_\omega (\mathbf{m} - \mathbf{m}_\mathcal{T}) \cdot (\mathbf{f} - \mathbf{f}_\mathcal{T}) \, dx \leq \| \, \nabla \mathbf{m} \, \|_{L^\infty(\omega)} \, \| \, h_\mathcal{T}(\mathbf{f} - \mathbf{f}_\mathcal{T}) \, \|_{L^1(\omega)}.$$

Note that $\| \, h_\mathcal{T}(\mathbf{f} - \mathbf{f}_\mathcal{T}) \, \|_{L^1(\Omega)} = \mathcal{O}(\| \, h_\mathcal{T} \, \|_\infty^2)$ is of optimal order. Finally, in the uniaxial case $\phi^{**}(\mathbf{m}) = (\mathbf{m} \cdot \mathbf{e}_\perp)^2/2$ and for an easy axis $\mathbf{e}$ perpendicular to the exterior magnetic field $\mathbf{f}$ pointwise almost everywhere, we have

$$\int_\omega (\mathbf{m} - \mathbf{m}_\mathcal{T}) \cdot (\mathbf{f} - \mathbf{f}_\mathcal{T}) \, dx$$

$$\leq \| \, (\mathbf{m} - \mathbf{m}_\mathcal{T}) \cdot \mathbf{e}_\perp \, \|_{L^2(\omega)} \, \| \, \mathbf{f} - \mathbf{f}_\mathcal{T} \, \|_{L^2(\Omega)}$$

$$(5.7) \qquad = \| \, D\phi^{\star\star}(\mathbf{m}) - D\phi^{\star\star}(\mathbf{m}_h) \, \|_{L^2(\omega)} \, \| \, \mathbf{f} - \mathbf{f}_\mathcal{T} \, \|_{L^2(\Omega)} \, ,$$

and $\| \, D\phi^{\star\star}(\mathbf{m}) - D\phi^{\star\star}(\mathbf{m}_h) \, \|_{L^2(\omega)}$ can be absorbed. This merely results in an additional term $\| \, \mathbf{f} - \mathbf{f}_\mathcal{T} \, \|_{L^2(\Omega)}^2$ on the right-hand side.
(ii) The estimate (5.2) plus (5.5) is reliable (i.e., the error is bounded from above by a constant times the computable bound).
(iii) The estimate (5.3) plus (5.5) is reliable in the sense that the constant c_8 does not depend on the regularity of $\mathbf{m}$ or ∇u. In case (5.2) plus (5.5) the constant c_7 does depend on the smoothness of the exact solution which is

uncertain. (The authors are unaware of any regularity results on $\mathbf{m}$.) Consequently, we have to regard (5.2) as non-reliable.

(iv) The estimate (5.3) is not efficient since the power of the jump contributions is one. This is different for (5.4) where all the terms on the right-hand side are of optimal order.

(v) The complementary properties of the error estimates suggest to employ (5.2) in an adaptive mesh-refining strategy but use (5.3) for reliable (but possibly expensive) error estimation.

(vi) Note that $|[\mathbf{m}_h - \nabla_\mathcal{T} u_h] \cdot n_\mathcal{E}|$ does not appear in (5.3) while $|[\partial u_h / \partial s]|$ is typical in a posteriori error estimates for nonconforming finite element schemes.

Proof of Theorem 5.2.   Throughout this proof, we abbreviate $e := u - u_h$, $\boldsymbol{\delta} := \mathbf{m} - \mathbf{m}_h$ and extend $\mathbf{m}$, $\mathbf{m}_h$, and $\boldsymbol{\delta}$ by zero outside of ω.

As in the first step of the proof of the a priori error estimates, we add (4.12) and (4.13) and substitute the resulting estimate for $(\lambda\mathbf{m} - \lambda_h\mathbf{m}_h) \cdot \boldsymbol{\delta}$ in (4.17) and so infer

$$\| \nabla_\mathcal{T} e \|_{2,\Omega}^2 + \int_\omega (D\phi^{**}(\mathbf{m}) - D\phi^{**}(\mathbf{m}_h)) \cdot \boldsymbol{\delta} \, dx$$

$$\leq \int_\omega (\mathbf{m} - \mathbf{m}_\mathcal{T}) \cdot (\mathbf{f} - \mathbf{f}_\mathcal{T}) dx + \int_\omega \varepsilon\lambda_h |\mathbf{m}_h| (\lambda|\mathbf{m}| - \lambda_h|\mathbf{m}_h|) dx$$

$$(5.8) \quad + \int_\Omega \nabla_\mathcal{T} e \cdot (\nabla_\mathcal{T} e - \boldsymbol{\delta}) dx,$$

where we added $\| \nabla_\mathcal{T} e \|_{2,\Omega}^2$ on both sides.

To bound the second term on the right-hand side of (5.8), we employ (2.6) resp. (3.9) to obtain expressions for $\lambda|\mathbf{m}|$ resp. $\lambda_h|\mathbf{m}_h|$ and subtract the two resulting formulae. This proves

$$\int_\omega \varepsilon\lambda_h |\mathbf{m}_h| (\lambda|\mathbf{m}| - \lambda_h|\mathbf{m}_h|) dx$$

$$\leq \int_\omega \varepsilon\lambda_h |\mathbf{m}_h| \big| \mathbf{f} - \mathbf{f}_\mathcal{T} - \nabla_\mathcal{T} \mathbf{e} - D\phi^{**}(\mathbf{m}) + D\phi^{**}(\mathbf{m}_h) \big| \, dx$$

$$\leq (1 + \frac{1}{2c_1}) \int_\omega \varepsilon^2 \lambda_h^2 |\mathbf{m}_h|^2 dx + \frac{1}{2} \| \mathbf{f} - \mathbf{f}_\mathcal{T} \|_{2,\omega_h}^2$$

$$(5.9) \quad + \frac{c_1}{2} \| D\phi^{**}(\mathbf{m}) - D\phi^{**}(\mathbf{m}_h) \|_{2,\omega_h}^2 + \frac{1}{2} \| \nabla_\mathcal{T} \mathbf{e} \|_{2,\omega_h}^2 .$$

For the last term on the right-hand side of (5.8) we first observe that $\nabla u - \mathbf{m}$ is divergence-free in the sense of distributions on Ω. Hence, there exists a function $b \in H^1(\Omega)$ with $\nabla u - \mathbf{m} = \text{curl } b := (\partial b / \partial x_2, -\partial b / \partial x_1)$.

Let b_h be the Clement-interpolation to b (no boundary conditions); b_h is continuous and $\mathcal{T}$-piecewise affine and, if $b \in H^{\beta+1}(\Omega)$, there holds

$$\| h_{\mathcal{T}}^{-\beta} \nabla(b - b_h) \|_{2,\Omega} + \| h_{\mathcal{T}}^{-(\beta+1)}(b - b_h) \|_{2,\Omega}$$

(5.10) $$+ \| h_{\mathcal{E}}^{-(\beta+1/2)}(b - b_h) \|_{2,\cup\mathcal{E}} \le c_{10} \,| b |_{\beta+1,2,\Omega}.$$

The constant $c_{10} > 0$ depends only on ω and the aspect ratio of the elements, but does not depend on their sizes (or on b or B) [Cl, BS, V]. An elementwise integration by parts shows

(5.11) $$\int_\Omega \operatorname{curl} B \cdot \nabla_{\mathcal{T}} u_h \, dx = \int_{\cup\mathcal{E}} [u_h] \operatorname{curl} B \cdot n \, ds = 0$$

since $\operatorname{curl} b_h \cdot n = \partial b_h / \partial s$ is continuous in the sense that there is no difference on both sides of E and $\operatorname{curl} b_h \cdot n$ is constant there while $[u_h]$ has a vanishing integral mean on E by construction of the Crouzeix-Raviart elements.

The discrete counterpart $\nabla_{\mathcal{T}} u_h - \mathbf{m}_h$ is perpendicular to $\nabla_{\mathcal{T}} u_h$ in $L^2(\Omega)$ according to (3.8). Surprisingly, $\nabla_{\mathcal{T}} u_h - \mathbf{m}_h$ is perpendicular to ∇u as well. Indeed, with the interpolation (4.7) and with (3.8), we deduce with an elementwise integration by parts that

$$\int_\Omega \nabla u \cdot (\nabla_{\mathcal{T}} u_h - \mathbf{m}_h) dx = \int_\Omega \nabla_{\mathcal{T}}(u - I_{\mathcal{T}} u) \cdot (\nabla_{\mathcal{T}} u_h - \mathbf{m}_h) dx$$

(5.12) $$= \int_{\cup\mathcal{E}} [(u - I_{\mathcal{T}} u)(\nabla_{\mathcal{T}} u_h - \mathbf{m}_h)] \cdot n_E \, ds.$$

(In the last step we used that $\mathbf{m}_h$ is $\mathcal{T}$-piecewise constant and u_h is $\mathcal{T}$-piecewise affine such that $\operatorname{div}_{\mathcal{T}}(\nabla_{\mathcal{T}} u_h - \mathbf{m}_h) = 0$.) For each edge $E \in \mathcal{E}$, $u - I_{\mathcal{T}} u$ has integral mean zero on E and $\nabla_{\mathcal{T}} u_h - \mathbf{m}_h$ is constant there. Hence, even if the corresponding quantities are discontinuous on E, we have

$$\int_\Omega \nabla_{\mathcal{T}} e \cdot (\nabla_{\mathcal{T}} u_h - \mathbf{m}_h) dx = \int_{\cup\mathcal{E}} [(u - I_{\mathcal{T}} u)(\nabla_{\mathcal{T}} u_h - \mathbf{m}_h)] \cdot n_E \, ds$$

(5.13) $$= 0.$$

From (5.11), (5.13), and $\nabla u - \mathbf{m} = \operatorname{curl} b$, we deduce with an elementwise integration by parts and Cauchy's inequality that

$$\int_\omega \nabla_{\mathcal{T}} e \cdot (\nabla_{\mathcal{T}} e - \boldsymbol{\delta}) dx = \int_\omega \nabla_{\mathcal{T}} e \cdot \operatorname{curl}(b - b_h) dx$$

$$= - \int_\omega \nabla_{\mathcal{T}} u_h \cdot \operatorname{curl}(b - b_h) dx$$

$$= - \int_{\cup\mathcal{E}} [\partial u_h / \partial s](b - b_h) dx$$

$$\leq \| \, h_{\mathcal{E}}^{-1/2}(b - b_h) \, \|_{2,\cup\mathcal{E}} \, \| \, h_{\mathcal{E}}^{1/2}[\partial u_h/\partial s] \, \|_{2,\cup\mathcal{E}}$$

(5.14)
$$\leq c_{10} \, | \, b \, |_{1,2,\Omega} \, \| \, h_{\mathcal{E}}^{1/2}[\partial u_h/\partial s] \, \|_{2,\cup\mathcal{E}}.$$

Notice that, for higher regularity of $b \in W^{2,\infty}(\Omega)$ and with its nodal inter-polant b_h the arguments in (5.14) show

(5.15)
$$\int_{\Omega} \nabla e \cdot (\nabla_{\mathcal{T}} e - \boldsymbol{\delta}) dx \leq c_{10} \, | \, b \, |_{2,\infty,\Omega} \, \| \, h_{\mathcal{E}}^2[\partial u_h/\partial s] \, \|_{1,\cup\mathcal{E}}.$$

In the final step we gather all the estimates on the right-hand side of (5.8) in (5.5), (5.9), (5.14), and (5.15) and eventually obtain,

$$\frac{1}{2} \| \, \nabla_{\mathcal{T}} e \, \|_{2,\Omega}^2 + \int_{\omega} (D\phi^{**}(\mathbf{m}) - D\phi^{**}(\mathbf{m}_h)) \cdot \boldsymbol{\delta} \, dx$$

$$\leq (1 + \frac{1}{2c_1}) \int_{\omega} \varepsilon^2 \lambda_h^2 |\mathbf{m}_h|^2 dx + \int_{\omega} (\mathbf{m} - \mathbf{m}_{\mathcal{T}}) \cdot (\mathbf{f} - \mathbf{f}_{\mathcal{T}}) dx$$

$$+ \frac{1}{2} \| \, \mathbf{f} - \mathbf{f}_{\mathcal{T}} \, \|_{2,\omega}^2 + \frac{c_1}{2} \| \, D\phi^{**}(\mathbf{m}) - D\phi^{**}(\mathbf{m}_h) \, \|_{2,\omega}^2$$

(5.16)
$$+ c_1 | \, b \, |_{1+\alpha,2,\omega} \| \, h_{\mathcal{E}}^{1/2}[\partial u_h/\partial s] \, \|_{2,\cup\mathcal{E}}.$$

Absorbing $|D\phi^{**}(\mathbf{m}) - D\phi^{**}(\mathbf{m}_h)|^2$ with (4.3), we conclude the proof of the theorem. We omitt details in the remaining case. $\qquad\square$

Proof of Theorem 5.1. Arguing as above we deduce (5.8) and estimate the first and second term on its right-hand side as in (5.5)-(5.9). The last term in (5.8) reads

(5.17)
$$\int_{\Omega} \nabla e \cdot (\nabla e - \boldsymbol{\delta}) dx = \int_{\Omega} \nabla(e - e_h) \cdot (\mathbf{m}_h - \nabla u_h) dx,$$

where $e_h \in \mathcal{S}_0^1(\mathcal{T})$ denotes the Clement-interpolation to e which satisfies estimates as in (5.10) (where b resp. b_h is replaced by $\mathbf{e}$ resp. $\mathbf{e_h}$). According to $\text{div}_{\mathcal{T}}(\mathbf{m}_h - \nabla u_h) = 0$, an integration by parts on the right-hand side in (5.17) shows

$$\int_{\Omega} \nabla e \cdot (\nabla e - \boldsymbol{\delta}) dx = \int_{\cup\mathcal{E}} (e - e_h)[\mathbf{m}_h - \nabla u_h] \cdot n_{\mathcal{E}} \, ds$$

(5.18)
$$\leq c_{10} \| \, \nabla e \, \|_2 \, \| \, h_{\mathcal{E}}^{1/2}[\mathbf{m}_h - \nabla u_h] \cdot n_{\mathcal{E}} \, \|_{2,\cup\mathcal{E}}.$$

The remaining parts in this proof are analogous to those in the previous and hence omitted. $\qquad\square$

6. Numerical realisation

Computational examples are provided for the uniaxial case (with the easy axis $\mathbf{e} \in \mathbb{R}^2$) to compare the conforming method and the nonconforming method with respect to stability as well as convergence properties. We consider the minor generalisation $(\tilde{P})$ of (P) on the right hand side of (6.1).

This is a small modification of Problem (P) stated in (2.5)–(2.7).

Problem $(\tilde{P})$: Given $(g, \mathbf{f}) \in L^2(\Omega) \times L^2(\omega)^2$, seek $(u, \mathbf{m}, \lambda) \in H_0^1(\Omega) \times L^2(\omega)^2 \times L^2(\omega)$ that satisfies, for all $w \in H_0^1(\Omega)$ and $\mu \in L^2(\omega)^2$,

(6.1) $\qquad \int_\Omega \nabla u \cdot \nabla w \, dx - \int_\omega \mathbf{m} \cdot \nabla w \, dx = \int_\Omega g \cdot w \, dx,$

$$\int_\omega \nabla u \cdot \mu \, dx + \int_\omega (\mathbf{m} \cdot \mathbf{e}_\perp)(\mu \cdot \mathbf{e}_\perp) \, dx + \int_\Omega \lambda \mathbf{m} \cdot \mu \, dx$$

(6.2) $\qquad = \int_\Omega \mathbf{f} \cdot \mu \, dx,$

(6.3) $\qquad 0 \le \lambda, \quad |\mathbf{m}| \le 1, \quad \text{and} \quad \lambda(1 - |\mathbf{m}|)_+ = 0 \quad \text{a.e. in } \omega,$

The side constraint $|\mathbf{m}| \le 1$ is enforced by a penalisation strategy and leads to Problem $(\tilde{P}_\varepsilon)$ and its conforming resp. nonconforming discretisation $(\tilde{P}_{\varepsilon,N})$ resp. $(\tilde{P}_{\varepsilon,N}^{NC})$ solved numerically by a Newton-Raphson scheme.

Let $\phi_1, .., \phi_J$ be hat functions for each vertex of elements $T \in \mathcal{T}$ in the conforming scheme resp. each edge in the nonconforming scheme. Furthermore, let $\psi_1, .., \psi_K$ be the characteristic functions, for each element in $\mathcal{T}|_\omega = \{T_1, .., T_K\}$. The iterates $u_h^{(\nu)} := \sum_{j=1}^{J} x_j^{(\nu)} \phi_j$ and $\mathbf{m}_h^{(\nu)} = (\sum_{k=1}^{K} y_k^{(\nu)} \psi_k, \sum_{k=1}^{K} y_{K+k}^{(\nu)} \psi_k)$ are assembled from $(x^{(\nu)}, y^{(\nu)}) \in \mathbb{R}^J \times \mathbb{R}^{2K}$. The implementation of the Newton-Raphson algorithm is performed in Matlab in the spirit of [ACF].

Algorithm 6.1. *Start, e.g., with $(x^{(0)}, y^{(0)}) := (0, 0)$, and solve or $\nu = 0, 1, 2, \ldots$ until termination if* $|(G^{(\nu)}, F^{(\nu)})| \le 10^{-12}$,

(6.4)
$$\begin{pmatrix} A & B \\ -B^\top & C + \frac{1}{\varepsilon}(D(y^{(\nu)}) + E(y^{(\nu)})) \end{pmatrix} \begin{pmatrix} x^{(\nu)} - x^{(\nu+1)} \\ y^{(\nu)} - y^{(\nu+1)} \end{pmatrix} = \begin{pmatrix} G^{(\nu)} \\ F^{(\nu)} \end{pmatrix},$$

where $H : \mathbb{R} \to \mathbb{R}_0^+$ is the Heaviside function, $1_{2\times2}$ is the 2×2-unit matrix, and for $j, \ell = 1, \ldots, J, k = 1, \ldots, K$,

(6.5) $\qquad\qquad\qquad A_{j\ell} = \int_\Omega \nabla_\mathcal{T} \phi_j \cdot \nabla_\mathcal{T} \phi_\ell \, dx,$

(6.6) $\qquad\qquad (B_{j,k}, B_{j,K+k}) = \int_\omega \psi_k \cdot \nabla_\mathcal{T} \phi_j \, dx,$

(6.7) $\begin{pmatrix} C_{k,k} & C_{k,K+k} \\ C_{K+k,k} & C_{K+k,K+k} \end{pmatrix} = |T_k|\, \mathbf{e}_\perp \otimes \mathbf{e}_\perp,$

$$\begin{pmatrix} D_{k,k} & D_{k,K+k} \\ D_{K+k,k} & D_{K+k,K+k} \end{pmatrix} = \frac{H(|(y_k^{(\nu)}, y_{K+k}^{(\nu)})| - 1)}{|(y_k^{(\nu)}, y_{K+k}^{(\nu)})|}$$

(6.8)
$$\times \begin{pmatrix} y_k^{(\nu)} \\ y_{K+k}^{(\nu)} \end{pmatrix} \otimes \begin{pmatrix} y_k^{(\nu)} \\ y_{K+k}^{(\nu)} \end{pmatrix},$$

(6.9) $\begin{pmatrix} E_{k,k} & E_{k,K+k} \\ E_{K+k,k} & E_{K+k,K+k} \end{pmatrix} = \left(|(y_k^{(\nu)}, y_{K+k}^{(\nu)})| - 1\right)_+ 1_{2\times 2},$

and the right-hand side of (6.4) with barycenters s_{T_k},

(6.10) $\begin{pmatrix} G^{(\nu)} \\ F^{(\nu)} \end{pmatrix} = \begin{pmatrix} A & B \\ -B^\top & C + \frac{1}{\varepsilon}E(y^{(\nu)}) \end{pmatrix} \begin{pmatrix} x^{(\nu)} \\ y^{(\nu)} \end{pmatrix} - \begin{pmatrix} G \\ F \end{pmatrix},$

(6.11) $G_j := \dfrac{1}{3} \displaystyle\sum_{T_\ell \subset \mathrm{supp}\phi_j} |T_\ell|\, g(s_{T_\ell}) \approx \int_\Omega g\phi_j\, dx,$

(6.12) $\begin{pmatrix} F_k \\ F_{K+k} \end{pmatrix} := |T_k|\, \mathbf{f}(s_{T_k}) \approx \displaystyle\int_\omega \mathbf{f}\psi_k\, dx.$

Remark 6.1. The algorithm is stabilised for $(P_{\varepsilon,N})$ to select exactly one of the possible solutions by adding the $2K \times 2K$-diagonal matrix

$\mathrm{diag}(|T_1|^{3/2}, \ldots, |T_K|^{3/2}, |T_1|^{3/2}, \ldots, |T_K|^{3/2})$, $|T_k|$ denotes the area of the element T_k, to the lower right block entry $C + \frac{1}{\varepsilon}(D(y^{(\nu)}) + E(y^{(\nu)}))$ in (6.4).

As in Theorem 5.1 and 5.2, we can prove the following bound for the uniaxial case and the conforming scheme $(P_{h_\mathcal{T},N})$, i.e., $\varepsilon = h_\mathcal{T}$,

(6.13)
$$\| \nabla(u - u_h) \|_{L^2(\Omega)} + \| (\mathbf{m} - \mathbf{m}_h) \cdot \mathbf{e}_\perp \|_{L^2(\omega)} \le \min\{c_{11}\eta_C^{(0)}, c_{12}\eta_C^{(1)}\},$$

and for the nonconforming method $(P_{h_\mathcal{T},N}^{NC})$,

$$\| \nabla_\mathcal{T}(u - u_h) \|_{L^2(\Omega)} + \| (\mathbf{m} - \mathbf{m}_h) \cdot \mathbf{e}_\perp \|_{L^2(\omega)}$$

(6.14)
$$\le \min\{c_{11}\eta_{NC}^{(0)}, c_{12}\eta_{NC}^{(1)}\},$$

where the constants c_{11}, c_{12} do not depend on h_T and the error estimators are, for $\beta = 0, 1$,

$$\eta_C^{(\beta)} := \left(\| h_\mathcal{T}\lambda_h\mathbf{m}_h \|_{L^2(\omega)}^2 + \| \mathbf{f} - \mathbf{f}_\mathcal{T} \|_{L^2(\omega)}^2 + \| h_\mathcal{T}^\beta(\mathbf{f} - \mathbf{f}_\mathcal{T}) \|_{L^1(\omega)} \right.$$

$$(6.15) \qquad +\| h_{\mathcal{T}} g \|_{L^2(\Omega)}^2 + \| h_{\mathcal{E}}^{1/2}[\mathbf{m}_h - \nabla u_h] \cdot n_{\mathcal{E}} \|_{L^2(\cup \mathcal{E})}^2 \Big)^{1/2},$$

$$\eta_{NC}^{(0)} := \Big(\| h_{\mathcal{T}} \lambda_h \mathbf{m}_h \|_{L^2(\omega)}^2 + \| \mathbf{f} - \mathbf{f}_{\mathcal{T}} \|_{L^2(\omega)}^2 + \| \mathbf{f} - \mathbf{f}_{\mathcal{T}} \|_{L^1(\omega)}$$

$$(6.16) \qquad +\| h_{\mathcal{T}} g \|_{L^2(\Omega)}^2 + \| h_{\mathcal{E}}^{1/2}[\partial u_h / \partial s] \|_{L^2(\cup \mathcal{E})} \Big)^{1/2},$$

$$\eta_{NC}^{(1)} := \Big(\| h_{\mathcal{T}} \lambda_h \mathbf{m}_h \|_{L^2(\omega)}^2 + \| \mathbf{f} - \mathbf{f}_{\mathcal{T}} \|_{L^2(\omega)}^2 + \| h_{\mathcal{T}}(\mathbf{f} - \mathbf{f}_{\mathcal{T}}) \|_{L^1(\omega)}$$

$$(6.17) \qquad +\| h_{\mathcal{T}} g \|_{L^2(\Omega)}^2 + \| h_{\mathcal{E}}^2[\partial u_h / \partial s] \|_{L^1(\cup \mathcal{E})} \Big)^{1/2}.$$

The estimates (6.15) resp. (6.18) motivate error indicators for local adaptive mesh-refinement, namely for $\beta = 0, 1$,

$$\eta_{T,C}^{(\beta)} := \Big(\| h_T \lambda_h \mathbf{m}_h \|_{L^2(T)}^2 + \| \mathbf{f} - \mathbf{f}_{\mathcal{T}} \|_{L^2(T)}^2 + \| h_{\mathcal{T}}^\beta (\mathbf{f} - \mathbf{f}_{\mathcal{T}}) \|_{L^1(T)}$$

$$(6.18) \qquad +\| h_{\mathcal{T}} g \|_{L^2(T)}^2 + \| h_{\mathcal{E}}^{1/2}[\mathbf{m}_h - \nabla u_h] \cdot n_{\mathcal{E}} \|_{L^2(\partial T)}^2 \Big)^{1/2},$$

$$\eta_{T,NC}^{(1)} := \Big(\| h_T \lambda_h \mathbf{m}_h \|_{2,T}^2 + \| \mathbf{f} - \mathbf{f}_{\mathcal{T}} \|_{L^2(T)}^2 + \| h_{\mathcal{T}}(\mathbf{f} - \mathbf{f}_{\mathcal{T}}) \|_{L^1(T)}$$

$$(6.19) \qquad +\| h_{\mathcal{T}} g \|_{L^2(T)}^2 + \| h_{\mathcal{E}}^2[\partial u_h / \partial s] \|_{L^1(\partial T)} \Big)^{1/2}.$$

Remarks 6.1. (i) Note that the a posteriori error estimates (6.15) resp. (6.18) are reliable for $\beta = 0$ in the sense that c_{11} does not depend on the data in contrast to c_{12} that depends on the (unknown) regularity of the exact solution. The estimates are efficient for $\beta = 1$ in the sense that the upper bounds have optimal convergence order.
(ii) The error estimator (6.16) is not a sum of local contributions. For the remaining estimators we have, for $\beta = 0, 1$,

$$(6.20) \qquad \eta_C^{(\beta)} = \big(\sum_{T \in \mathcal{T}} (\eta_{T,C}^{(\beta)})^2 \big)^{1/2} \quad \text{and} \quad \eta_{NC}^{(1)} = \big(\sum_{T \in \mathcal{T}} (\eta_{T,NC}^{(1)})^2 \big)^{1/2}.$$

For any choice of $\eta_T = \eta_{T,C}^{(0)}, \eta_{T,C}^{(1)}$ and $\eta = \eta_C^{(0)}, \eta_C^{(1)}$ resp. $\eta_T = \eta_{T,NC}^{(1)}$ and $\eta = \eta_{NC}^{(0)}, \eta_{NC}^{(1)}$, the subsequent mesh-refining algorithm generates a sequence $\mathcal{T}_0, \mathcal{T}_1, ...$ of adapted meshes.

Algorithm 6.2. *1. Start with coarse mesh $\mathcal{T}_0$.*
2. Solve the discrete problem with respect to $\mathcal{T}_k$.
3. Compute η_T for all $T \in \mathcal{T}_k$.
4. Compute error bound η and terminate or goto 5.
5. Mark element T red iff $\eta_T \geq \frac{1}{2} \max_{K \in \mathcal{T}_k} \eta_K$.
6. Red-green-blue-refinement (cf., e.g., [V]) to avoid hanging nodes, generate mesh $\mathcal{T}_{k+1}$, set $k = k + 1$ and goto 2.

7. Numerical examples

7.1. Academic example for numerical justification of theoretical results

The first example provides experimental evidence for the optimal choice of the penalty parameter $\varepsilon = h^\beta$, $\beta > 0$, and discusses its influence onto the number of iteration steps in Algorithm 1. Stability properties and mesh-dependencies as well as convergence analyses are studied for $(\tilde{P}_{\varepsilon,N})$ and $(\tilde{P}^{NC}_{\varepsilon,N})$.

Let $\omega = (1/4, 3/4)^2 \subset \Omega = (0,1)^2$, $\omega_1 := \{(x,y) \in \omega : 1 \leq \sin(2\pi(x - .25))\sin(2\pi(y - .25))\}$, and $\mathbf{e} = (e_1, e_2)$, and define

$$(7.1) \quad f(x,y) = \begin{cases} \begin{aligned} &\pi\left(\cos(\pi x)\sin(\pi y), \sin(\pi x)\sin(\pi y)\right) \\ &+(e_1 - e_2)\mathbf{e}_\perp \\ &+5\left((x - 3/2)^2 + (y - 1/2)^2\right) \quad &\text{if } (x,y) \in \omega_1, \\[6pt] &\pi\left(\cos(\pi x)\sin(\pi y), \sin(\pi x)\sin(\pi y)\right) \\ &+5\sin(2\pi(x - .25)) \\ &\times\sin(2\pi(x - .25))\,(e_1 - e_2)\mathbf{e}_\perp \quad &\text{if (x,y)} \notin \omega_1, \end{aligned} \end{cases}$$

$$(7.2) \quad g(x,y) = \begin{cases} 2\pi^2\sin(\pi x)\sin(\pi y) \quad &\text{if } (x,y) \in \omega_1 \cup (\Omega \setminus \omega), \\[6pt] \begin{aligned} &2\pi^2\sin(\pi x)\sin(\pi y) \\ &+10\pi\cos(2\pi(x - 1/4)) \\ &\times\sin(2\pi(y - 1/4)) \\ &+10\pi\sin(2\pi(x - 1/4)) \\ &\times\cos(2\pi(y - 1/4)) \quad &\text{if } (x,y) \in \omega \setminus \omega_1. \end{aligned} \end{cases}$$

Then, the solution $(u, \mathbf{m}, \lambda) \in H^1_0(\Omega) \times L^2(\omega)^2 \times L^2(\omega)$ of Problem $(\tilde{P})$ is given by

$$(7.3) \qquad u(x,y) = \sin(\pi x)\sin(\pi y) \quad \text{and} \quad \mathbf{m} = (\tilde{m}, \tilde{m}),$$

(7.4)
$$\tilde{m}(x,y) = \begin{cases} 1 & \text{if } (x,y) \in \omega_1, \\ 5\sin(2\pi(x - 1/4))\sin(2\pi(y - 1/4)) & \text{if } (x,y) \in \omega_1, \end{cases}$$

(7.5)
$$\lambda(x,y) = \begin{cases} 5\left((x - 3/2)^2 + (y - 1/2)^2\right) & \text{if } (x,y) \in \omega_1, \\ 0 & \text{if } (x,y) \in \omega \setminus \omega_1. \end{cases}$$

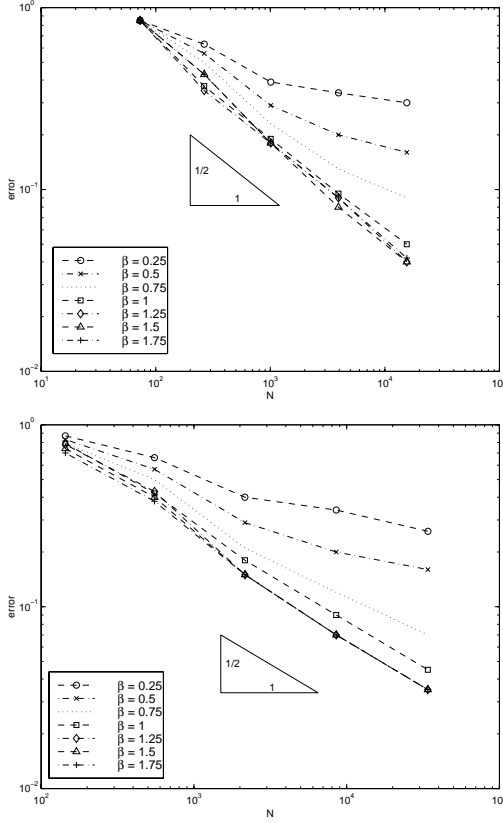In order to study the effect of penalisation in $(\tilde{P}^{NC}_{\varepsilon,N})$ and $(\tilde{P}_{\varepsilon,N})$, Fig. 2 displays errors $||\nabla(u - u_h)||_{L^2(\Omega)} + ||(\mathbf{m} - \mathbf{m}_h) \cdot \mathbf{e}_\perp||_{L^2(\omega)}$ versus the degrees of freedom N for different choices of $\varepsilon = h^\beta_{\mathcal{T}}$, $\beta = 0.25, .., 1.75$, where $\mathbf{e} = (1, 0)$. We added triangles to the plots to indicate the order of

Fig. 2. Error $= ||\nabla(u - u_h)||_{L^2(\Omega)} + ||(\mathbf{m} - \mathbf{m}_h) \cdot \mathbf{e}_\perp||_{L^2(\omega)}$ versus degrees of freedom N in $(\tilde{P}_{\varepsilon,N})$ (top) and $(\tilde{P}_{\varepsilon,N}^{NC})$ (bottom) with $\varepsilon = h^\beta$ on a uniform mesh for $\beta = .25, .5, .75, 1, 1.25, 1.5, 1.7$ in the first example

convergence which is twice the negative slope. In both pictures, the convergence improves if β increases from .25 to 1.0. The convergence behaviour for $\beta = 1.0, 1.25, 1.5$, and 1.75 is similar. On the other hand, the computational effort (counted in number of iterations in Algorithm 6.1) increases for higher values of β, see Fig. 3, which favours the optimal choice $\beta = 1$. Hence, we choose $\varepsilon = h_{\mathcal{T}}$ in all subsequent computations.

To study the mesh-dependency of the solutions in $(\tilde{P}_{h_{\mathcal{T}},N})$, we run Algorithm 6.1 on a uniform mesh with diagonals parallel to $\mathbf{e} = (1,1)/\sqrt{2}$ (aligned) or perpendicular for $\mathbf{e} = (-1,1)/\sqrt{2}$ (nonaligned). The Fig. 4 shows the approximate magnetisation $\mathbf{m}_h$ obtained by the conforming (top) and the nonconforming (bottom) scheme, with $\tilde{m}(x,y) = 0.8\sin(2\pi(x - 1/4))\sin(2\pi(y - 1/4))$ if $(x,y) \in \omega$ instead of (7.4) such that $\lambda = 0$ in (7.3)–(7.5) and instabilities might be enforced. While the right picture shows a reasonable approximation, the left picture indicates instabilities.
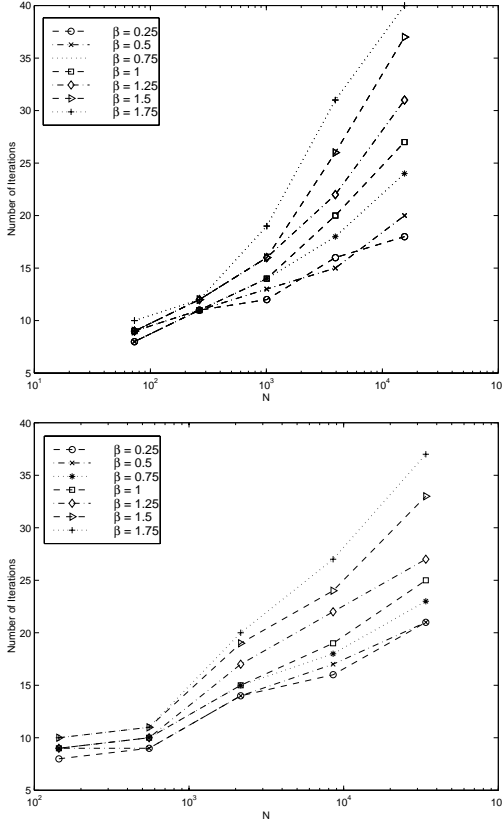
Fig. 3. Number of iteration steps in Algorithm 1, for solving $(\tilde{P}_{\varepsilon,N})$ (top) and $(\tilde{P}_{\varepsilon,N}^{NC})$ (bottom) with $\varepsilon = \mathcal{O}(h^{\beta})$ for different values of β in the first example

To assess the quality of the approximation, we show in Fig. 5 the components of the error $\mathbf{m} - \mathbf{m}_h$ in the direction $\mathbf{e}_{\perp}$ (for which we proved error estimates) and in the direction $\mathbf{e}$ (for which any control lacks). The result in Fig. 5 supports that $\|\mathbf{m} - \mathbf{m}_h\|$ does not converge to zero as discussed in Example 3.1. Note that the components in $\mathbf{e}_{\perp}$-direction converge with experimental convergence rates close to 1.

To study the practical performance of the a posteriori error indicators for uniform and adapted meshes generated by Algorithm 6.2, Fig. 6 resp. 7 show the convergence rates for the estimated error contributions (top) and the uncontrolled magnetisation error $\|\mathbf{m} - \mathbf{m}_h\|_{L^2(\omega)}$ (bottom) and some error estimators (6.20) for the conforming (Fig. 6) and the nonconforming scheme (Fig. 7) on uniform and adapted meshes. In these figures, a label "$\eta^{(0)}$ ($\eta^{(1)}$-adapted)" indicates that the corresponding symbol displays $\eta^{(0)}$ versus the number of degrees of freedom N, for a sequence $\mathcal{T}_0, \mathcal{T}_1, ..,$ gener-
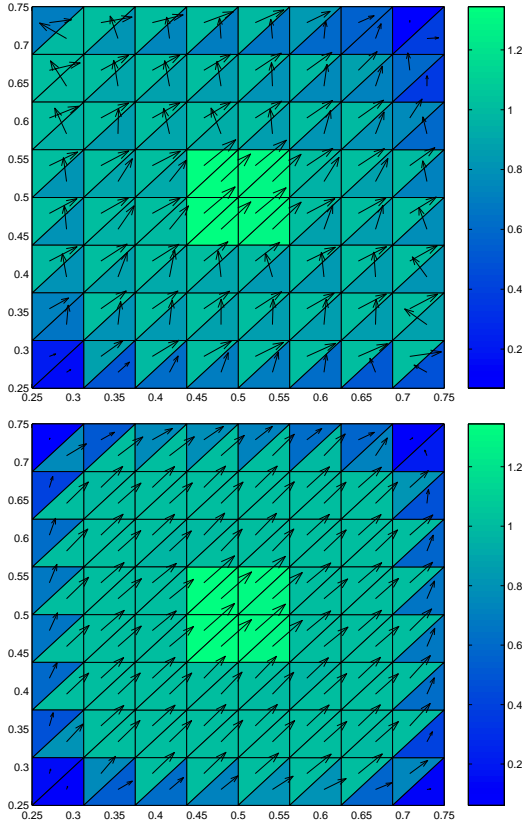
Fig. 4. Plot of computed magnetisation of $(\tilde{P}_{h,233})$ (top) and $(\tilde{P}_{h,520}^{NC})$ (bottom) for uniformly refined meshes in the first example. The gray-scale shows the modulus of the magnetisation
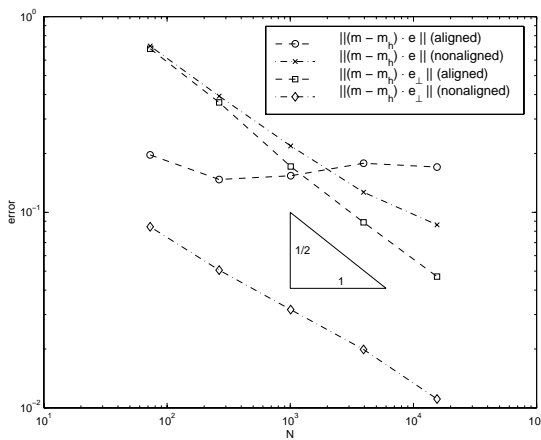

Fig. 5. Errors $||(\mathbf{m}-\mathbf{m}_h)\cdot\mathbf{e}_\perp||_{L^2(\omega)}$ versus degrees of freedom N in $(P_{h_\mathcal{T},N})$ for aligned and nonaligned meshes in the first example
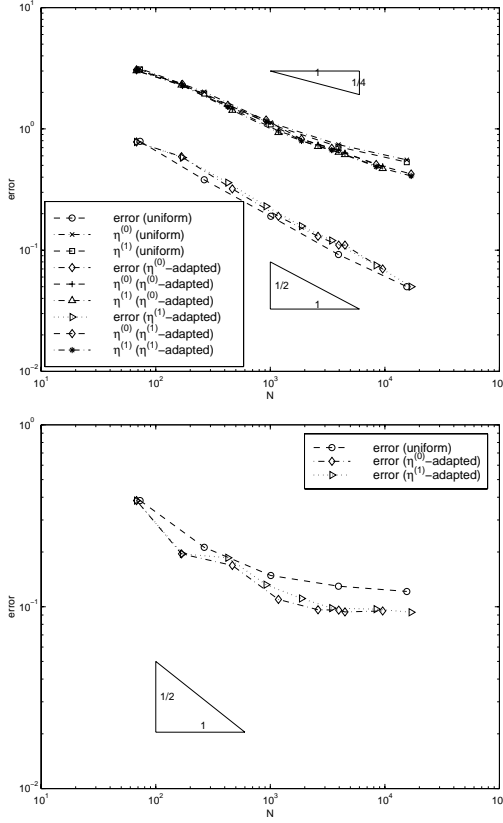
Fig. 6. Error $= ||\nabla(u - u_h)||_{L^2(\Omega)} + ||(\mathbf{m} - \mathbf{m}_h) \cdot \mathbf{e}_\perp||_{L^2(\omega)}$ (top) and error $= ||(\mathbf{m} - \mathbf{m}_h) \cdot \mathbf{e}||_{L^2(\omega)}$ (bottom) and error estimators $\eta = \eta_C^{(\beta)}$ versus degrees of freedom N in $(\tilde{P}_{h,N})$ for uniform and $\eta_C^{(\beta)}$-generated meshes in the first example

ated by Algorithm 6.2 with the error indicator $\eta_T^{(1)}$ in step 5. We observe an experimental convergence rate $1/2$ for reliable error estimators with $\beta = 0$ and also for the efficient error estimators with $\beta = 1$. To our surprise, the "efficient" error estimators for $\beta = 1$ do not reflect the experimental linear convergence of the true errors. This is rather pessimistic as the true errors converge linearly. The uncontrolled error $\| \mathbf{m} - \mathbf{m}_h \|_{L^2(\omega)}$ does not seem to converge for the conforming discretisation. A linear experimental convergence is deduced for all error components from Fig. 7 for the nonconforming schemes. The different convergence properties of $\eta_{NC}^{(\beta)}$ are expected at rate $1/2$ for $\beta = 0$ and rate 1 for $\beta = 1$. Also, the meshes generated by Algorithm 6.2 seem to be slightly better than a uniform discretisation. However, since the exact solution is Lipschitz continuous and at least piecewise smooth, the use of adapted meshes is not important in this example.
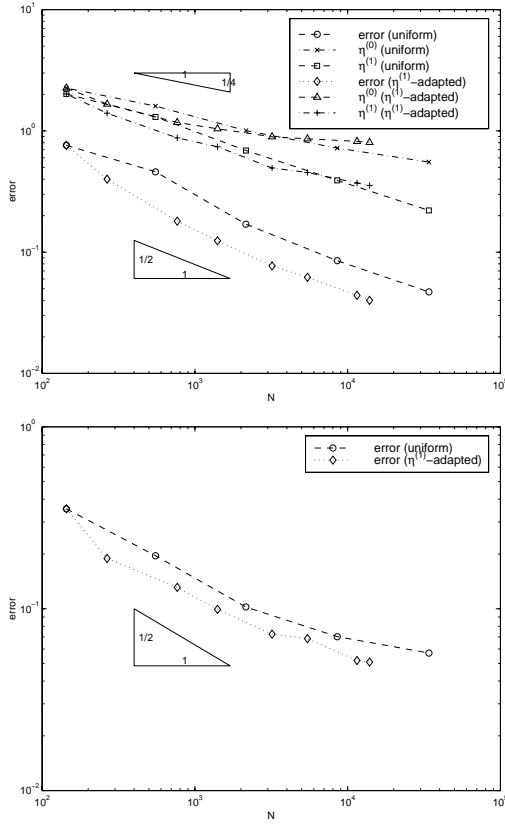
Fig. 7. Error $= ||\nabla_{\mathcal{T}}(u - u_h)||_{L^2(\Omega)} + ||(\mathbf{m} - \mathbf{m}_h) \cdot \mathbf{e}_\perp||_{L^2(\omega)}$ (top) and error $= ||(\mathbf{m} - \mathbf{m}_h) \cdot \mathbf{e}||_{L^2(\omega)}$ (bottom) and error estimators $\eta = \eta_{NC}^{(\beta)}$ versus degrees of freedom N in $(\tilde{P}_{h,N}^{NC})$ for uniform and $\eta_{NC}^{(1)}$-generated meshes in the first example
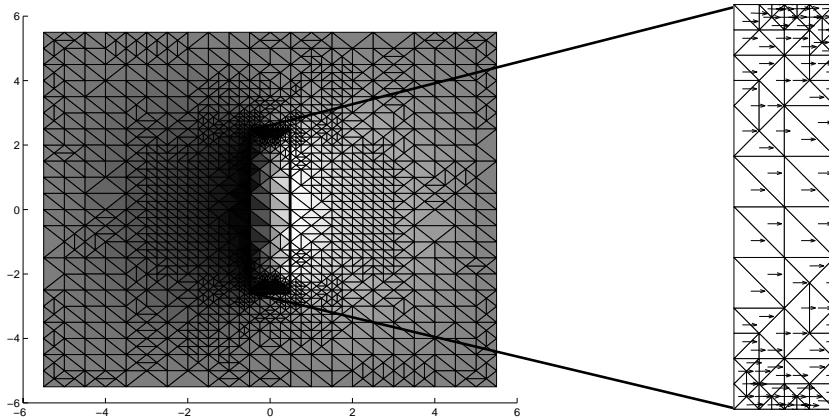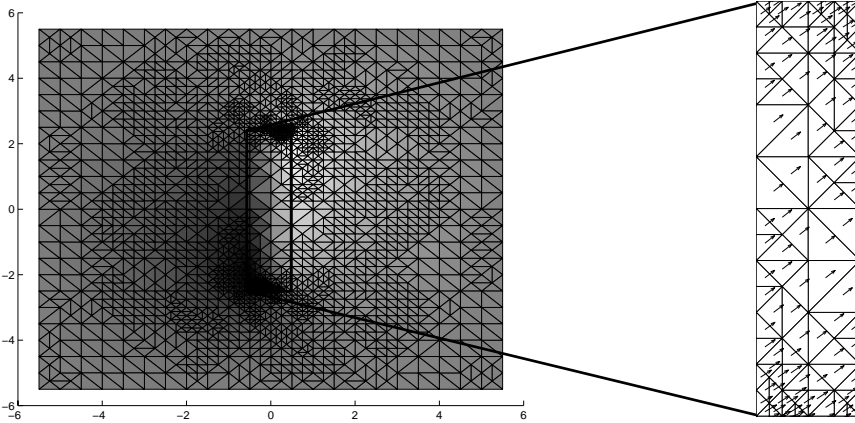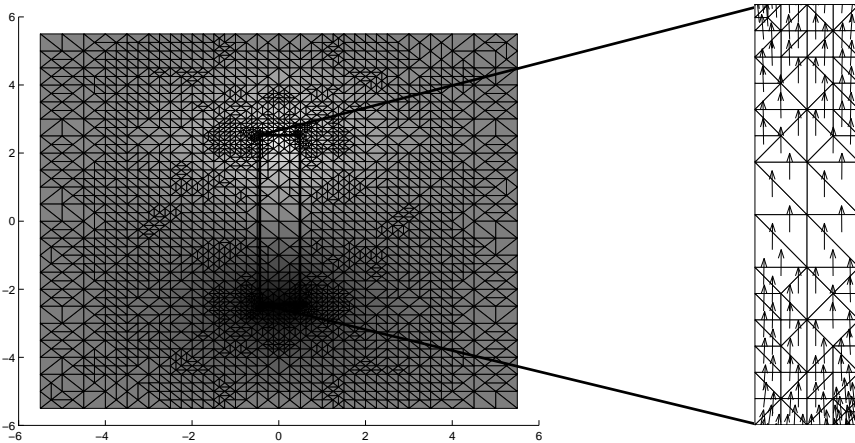

Fig. 8. Magnetic potential u_h (left) and magnetisation $\mathbf{m}_h$ (right) in a ferromagnetic rod, for $(P_{h_{\mathcal{T}},5444}^{NC})$ on $\eta_{NC}^{(1)}$-generated meshes, for $\mathbf{f} = (.6, 0) \parallel \mathbf{e} = (1, 0)$ in the second example

Fig. 9. Magnetic potential u_h (left) and magnetisation $\mathbf{m}_h$ (right) in a ferromagnetic rod, for $(P^{NC}_{h_{\mathcal{T}},7874})$ on $\eta^{(1)}_{NC}$-generated meshes, for $\mathbf{f} = (.5,.5)$ and $\mathbf{e} = (1,0)$ in the second example

Fig. 10. Magnetic potential u_h (left) and magnetisation $\mathbf{m}_h$ (right) in a ferromagnetic rod, for $(P^{NC}_{h_{\mathcal{T}},7284})$ on $\eta^{(1)}_{NC}$-generated meshes, for $\mathbf{f} = (0,.9) \perp \mathbf{e} = (1,0)$ in the second example

7.2. Scientific computing of an uniaxial ferromagnet under a constant magnetisation

The uniaxial ferromagnet covers the domain $\omega = (-.5,.5) \times (-2.5, 2.5) \subset\subset \Omega = (-5.5, 5.5)^2$. It is magnetised by an exterior field $\mathbf{f} = (.6, 0)$, $\mathbf{f} = (.5,.5)$, resp. $\mathbf{f} = (0,.9)$ and $\mathbf{e} = (1,0)$. The numerical results for $(P^{NC}_{h_{\mathcal{T}},N})$ on $\eta^{(1)}_{NC}$-generated meshes are displayed in Fig. 8, 9, resp. 10 for three choices of $\mathbf{f}$.
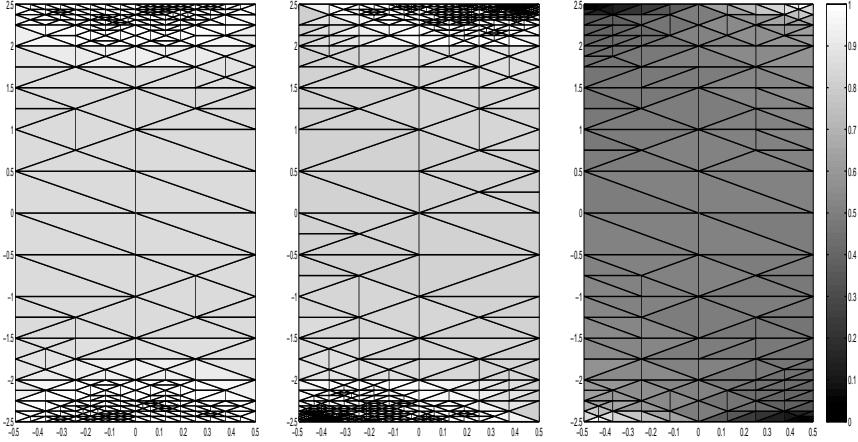
Fig. 11. Approximate volume fraction λ of related Young measures ν_x in (2.8) for Problem (M_0) for situations of Fig. 8 (left), Fig. 9 (middle), resp. Fig. 10 (right)
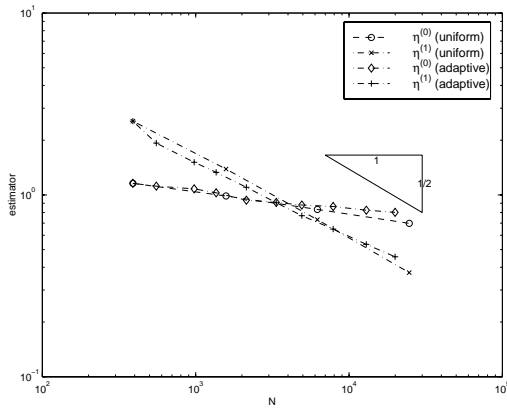

Fig. 12. Error estimators $\eta_{NC}^{(\beta)}$ versus degrees of freedom N in $(P_{h_\mathcal{T},N}^{NC})$ for uniform and $\eta_{NC}^{(1)}$-generated meshes in the second example (cf. Fig. 9)

According to the angle between the easy axis vector $\mathbf{e}$ and the constant exterior field $\mathbf{f}$, we arrive at different magnetisations and potential functions. The slightly different choices of $|\mathbf{f}|$ were made to obtain an intermediate non-fully saturated state with microstructures as indicated in Fig. 11.

In the first situation, $\mathbf{e} \parallel \mathbf{f}$ and $\mathbf{m}_h$ is almost uniformly following $\mathbf{f}$ with peak values of the modulus of $\mathbf{m}_h$ forming a cone-like structure at the bottom and the top of the ferromagnet. For $\sphericalangle(\mathbf{e}, \mathbf{f}) = \pi/4$ in the second situation, $\mathbf{m}_h$ mimics the direction of $\mathbf{f}$ but is inhomogeneous. The cone-like structure of peak values of $|\mathbf{m}_h|$ is now distorted. In the final case, a flower-like structure can be observed, with magnetisation of large modulus

concentrated at the edge points. Note that $\mathbf{f} \perp \mathbf{e}$ so that we could improve the a posteriori error estimates with Remark 5.1 (i).

The Young measure of the original Problem (M_0) is computed with (2.8)–(2.9) where $\mathbf{m}$ is replaced by $(\max(1, |\mathbf{m}_h|))^{-1}\mathbf{m}_h$. Fig. 11 displays the obtained approximations for the coefficient λ in the second examples shown in Fig. 8–10. Note that we described no error estimate for the approximation to ν_x (which is linked to the lack of control on $(\mathbf{m} - \mathbf{m}_h) \cdot \mathbf{e}$). Nevertheless, there is a weak convergence of the approximations and we conjecture that the approximation is accurate on a macroscopic level.

To assess the discretisation errors in the approximations of Fig. 8, 9, and 10, we computed $\eta_{NC}^{(\beta)}$. Since they show almost identical behavior in the three examples, we only plot the values for the second situation (Fig. 9) in Fig. 12. The error estimates show an experimental convergence rate 1 for $\beta = 1$ but a modest convergence behavior for $\beta = 0$.

References

[ACF] J. Alberty, C. Carstensen, S.A. Funken, Remarks around 50 lines of Matlab: Finite Element implementation, Numerical Algorithms (1999) Accepted, and: Berichtsreihe des Mathematischen Seminars Kiel **98–11** (1998) (http://www.numerik.uni-kiel.de/reports/1998/98-11.html)

[AF]   D. N. Arnold, R. S. Falk, A uniformly accurate finite element method for the Mindlin-Reissner plate, SIAM J. Numer. Anal. **26** (1989), 1276–1290

[BBF] F. Brezzi, K.-J. Bathe, M. Fortin, Mixed-interpolated elements for Reissner-Mindlin plates, Int. J. Num. Meth. Eng. **28** (1989), 1787–1801

[BF]   F. Brezzi, M. Fortin, Mixed and hybrid finite element methods, Springer-Verlag, 1991

[BS]   S.C. Brenner, L.R. Scott, The mathematical theory of finite element methods, Texts in Applied Mathematics **15**, Springer-Verlag, New York, 1994

[B]   W.F. Brown, Micromagnetics, Interscience, New York, 1963

[CP1] C. Carstensen, Petr Plecháč, Numerical solution of the scalar double-well problem allowing microstructure, Math. Comp. **66** (1997), 997–1026

[CP2] C. Carstensen, Petr Plecháč, Numerical Analysis of Compatible Phase Transitions in Elastic Solids, SIAM J. Numer. Anal. **37** (2000), 2061–2081

[Cl]   P. Clément, Approximation by finite element functions using local regularization, Sér. Rouge Anal. Numér. (RAIRO) **R-2** (1975), 77–84

[D]   B. Dacorogna, Direct Methods in the Calculus of Variations, Applied Math. Sciences **78**, Springer-Verlag, Heidelberg, 1989

[ADS] A. De Simone, Energy Minimizers for Large Ferromagnetic Bodies, Arch. Rat. Mech. Anal. **125** (1993), 99–143

[GR]   V. Girault, P.- A. Raviart, Finite Element Methods for Navier-Stokes Equations, Springer-Verlag, Berlin–Heidelberg–New York–Tokyo, 1986

[HS]   A. Hubert, R. Schäfer, Magnetic Domains – The Analysis of Magnetic Microstructures, Springer-Verlag, Berlin–Heidelberg–New York–Tokyo, 1998

[JK]   R. D. James, D. Kinderlehrer, Frustration in ferromagnetic materials, Continuum Mech. Thermodyn. **2** (1990), 215–239

[KR]   M. Kružík, T. Roubíček, Weierstrass-type maximum principle for microstructure in micromagnetics, Preprintreihe des des Max-Planck-Instituts für Mathematik in den Naturwissenschaften Leipzig **99–40** (1999)

[LM]   M. B. Luskin, L. Ma, Analysis of the finite element approximation of microstructure in micromagnetics, SIAM J. Numer. Anal. **29** (1992), 320–331

[P1]   P. Pedregal, Parametrized Measures and Variational Principles, Birkhäuser, 1997

[P2]   P. Pedregal, *Numerical computation of parametrized measures*, Numer. Funct. Anal. Opt. **16** (1995), 1049–1066

[P3]   P. Pedregal, On the numerical analysis of nonconvex variational problems, Num. Math. **74** (1996), 325–336

[Pr]   A. Prohl, Error analysis for the computation of microstructure in uniaxial ferromagnets, Berichtsreihe des Mathematischen Seminars Kiel **98–33** (1999) (`http://www.numerik.uni-kiel.de/reports/1998/98-33.html`)

[R]   T. Roubíček, Relaxation in Optimization Theory and Variational Calculus, W. de Gruyter, Berlin–New York, 1997

[T]   L. Tartar, Beyond Young Measures, Meccanica **30** (1995), 505–526

[V]   R. Verfürth, A review of a posteriori error estimation and adaptive mesh-refinement techniques, Wiley-Teubner, 1996